



This is a repository copy of *Measurements of $W+W^-$ production in decay topologies inspired by searches for electroweak supersymmetry*.

White Rose Research Online URL for this paper:
<https://eprints.whiterose.ac.uk/202424/>

Version: Published Version

Article:

Aad, G. orcid.org/0000-0002-6665-4934, Abbott, B. orcid.org/0000-0002-5888-2734, Abbott, D.C. orcid.org/0000-0002-7248-3203 et al. (2881 more authors) (2023) Measurements of $W+W^-$ production in decay topologies inspired by searches for electroweak supersymmetry. The European Physical Journal C, 83. 718.

<https://doi.org/10.1140/epjc/s10052-023-11508-9>

Reuse

This article is distributed under the terms of the Creative Commons Attribution (CC BY) licence. This licence allows you to distribute, remix, tweak, and build upon the work, even commercially, as long as you credit the authors for the original work. More information and the full terms of the licence here:
<https://creativecommons.org/licenses/>

Takedown

If you consider content in White Rose Research Online to be in breach of UK law, please notify us by emailing eprints@whiterose.ac.uk including the URL of the record and the reason for the withdrawal request.



eprints@whiterose.ac.uk
<https://eprints.whiterose.ac.uk/>



Measurements of W^+W^- production in decay topologies inspired by searches for electroweak supersymmetry

ATLAS Collaboration*

CERN, 1211 Geneva 23, Switzerland

Received: 1 July 2022 / Accepted: 9 October 2022
© CERN for the benefit of the ATLAS collaboration 2023

Abstract This paper presents a measurement of fiducial and differential cross-sections for W^+W^- production in proton–proton collisions at $\sqrt{s} = 13$ TeV with the ATLAS experiment at the Large Hadron Collider using a dataset corresponding to an integrated luminosity of 139 fb^{-1} . Events with exactly one electron, one muon and no hadronic jets are studied. The fiducial region in which the measurements are performed is inspired by searches for the electroweak production of supersymmetric charginos decaying to two-lepton final states. The selected events have moderate values of missing transverse momentum and the ‘stransverse mass’ variable m_{T2} , which is widely used in searches for supersymmetry at the LHC. The ranges of these variables are chosen so that the acceptance is enhanced for direct W^+W^- production and suppressed for production via top quarks, which is treated as a background. The fiducial cross-section and particle-level differential cross-sections for six variables are measured and compared with two theoretical SM predictions from perturbative QCD calculations.

1 Introduction

Measurements of W^+W^- (referred to hereafter as WW) production provide important tests of the electroweak (EWK) gauge structure of the Standard Model (SM) of particle physics, and WW production is also an important background process in searches for physics beyond the SM (BSM physics). In searches for supersymmetry [1–6] (SUSY) where WW events are a significant background, a semi-data-driven approach is often taken, that involves normalising the simulated Monte Carlo (MC) samples to data in a control region (CR), designed to be kinematically similar to the search regions but enriched in SM WW production. Significant deviations of these scaling factors from unity suggest mismodelling in the phase space targeted by the search, but it can be difficult to make comparisons with the level of agreement observed in precision SM measurements because

the scaling factors refer to detector-level quantities which are subject to mis-measurement and inefficiency. Producing ‘unfolded’ particle-level measurements, which are corrected for these effects and can directly be compared with the prediction of a MC event generator, in event topologies associated with search results is a novel way to address this whilst simultaneously extending the programme of precision SM measurements at the LHC. The ATLAS experiment [7] has previously reported differential measurements of $t\bar{t}$ and Z +jets production in regions related to a search for leptoquarks in dilepton+dijet events [8]. This paper presents the first effort to measure WW production cross-sections in topologies associated with SUSY searches.

Inclusive and fiducial WW production cross-sections have been measured in proton–proton (pp) collisions at $\sqrt{s} = 7$ TeV [9,10], 8 TeV [11–13] and 13 TeV [14–17] at the LHC, as well as in e^+e^- collisions at LEP [18] and in $p\bar{p}$ collisions at the Tevatron [19–21]. This analysis complements existing ATLAS measurements of WW production at 13 TeV in 0-jet events [15] and in ≥ 1 -jet events [16] by measuring differential cross-sections in a fiducial region kinematically close to the WW control region used in a previous search for electroweak production of supersymmetric charginos or sleptons [22]. That search targeted electroweak production of SUSY particles decaying into final states with two leptons (electrons or muons) and missing transverse momentum using 139 fb^{-1} of pp collisions at 13 TeV collected during Run 2 of the LHC and is referred to hereafter as the ‘EWK $2\ell+0$ -jets search’. In that search, WW production was the main background process and the associated theoretical uncertainties were among the dominant systematic uncertainties in the search regions. The present measurement targets event topologies with higher values of the dilepton invariant mass, $m_{e\mu}$, and the magnitude of the missing transverse momentum, E_T^{miss} , than were used in previous measurements, and can thus be used to provide additional constraints on BSM physics, and probe the expected SM backgrounds for future searches.

* e-mail: atlas.publications@cern.ch

The $WW \rightarrow e^\pm \nu \mu^\mp \nu$ decay channel is studied in events with no identified jets with a transverse momentum $p_T > 20$ GeV and pseudorapidity $|\eta| < 2.4$,¹ and with E_T^{miss} between 60 and 80 GeV. Missing transverse momentum is calculated so as to represent the momentum imbalance in the plane transverse to the colliding beams. High values of E_T^{miss} can be produced when weakly interacting neutral particles escape the detector unseen, and E_T^{miss} is thus an important variable in many BSM searches. This analysis also imposes requirements on the dilepton invariant mass that are more stringent than those in the $36 \text{ fb}^{-1} WW+0$ -jet measurement [15]. The dominant background process is top-quark production ($t\bar{t}$ and single-top Wt), which is estimated using the same data-driven method as was used in the EWK $2\ell+0$ -jets search. The measurements are performed in a fiducial phase space close to the geometric and kinematic acceptance of the experimental analysis. Differential cross-section measurements are performed for six variables, which are the same as those considered in the $36 \text{ fb}^{-1} WW+0$ -jet measurement [15]:

- The rapidity of the dilepton system, $|y_{e\mu}|$.
- The azimuthal separation between the two leptons, $|\Delta\phi_{e\mu}|$.
- The angular variable $\cos\theta^* = |\tanh(\Delta y(e\mu)/2)|$, which is longitudinally boost invariant and sensitive to the spin structure of the produced dileptons [23], and where $\Delta y(e\mu)$ is the difference between the electron and muon rapidities.
- The transverse momentum of the leading lepton, $p_T^{\text{lead}\ell}$.
- The invariant mass of the dilepton system, $m_{e\mu}$.
- The transverse momentum of the dilepton system, $p_T^{e\mu}$.

In this paper, $|y_{e\mu}|$, $|\Delta\phi_{e\mu}|$ and $\cos\theta^*$ are referred to collectively as ‘angular’ variables, as they probe angular correlations and are sensitive to the spin structure of the WW production system, and $p_T^{\text{lead}\ell}$, $m_{e\mu}$ and $p_T^{e\mu}$ are referred to collectively as ‘scale’ variables, as they characterise the energy scale of the process.

The rest of this paper is structured as follows. First, Sect. 2 describes the ATLAS detector and then Sect. 3 presents the analysis that is performed to measure the fiducial and differential cross-sections. This includes the data and MC samples used, the reconstructed-object definitions and event selections used to define the detector-level signal regions, and the SM background estimation, as well as the systematic uncer-

tainties considered and the unfolding techniques used to correct detector-level information back to particle level. Finally, the results are reported in Sect. 4, and Sect. 5 presents the conclusions.

2 ATLAS detector

The ATLAS experiment at the LHC is a multipurpose particle detector with a forward–backward symmetric cylindrical geometry and a near 4π coverage in solid angle. It consists of an inner tracking detector surrounded by a thin superconducting solenoid providing a 2 T axial magnetic field, electromagnetic and hadron calorimeters, and a muon spectrometer. The inner tracking detector covers the pseudorapidity range $|\eta| < 2.5$. It consists of silicon pixel, silicon microstrip, and transition radiation tracking detectors. Lead/liquid-argon (LAr) sampling calorimeters provide electromagnetic (EM) energy measurements with high granularity. A steel/scintillator-tile hadron calorimeter covers the central pseudorapidity range ($|\eta| < 1.7$). The endcap and forward regions are instrumented with LAr calorimeters for both the EM and hadronic energy measurements up to $|\eta| = 4.9$. The muon spectrometer surrounds the calorimeters and is based on three large superconducting air-core toroidal magnets with eight coils each. The field integral of the toroids ranges between 2.0 and 6.0 T across most of the detector. The muon spectrometer includes a system of precision tracking chambers and fast detectors for triggering. A two-level trigger system is used to select events. The first-level trigger is implemented in hardware and uses a subset of the detector information to accept events at a rate below 100 kHz. This is followed by a software-based trigger that reduces the accepted event rate to 1 kHz on average depending on the data-taking conditions. An extensive software suite [24] is used in the reconstruction and analysis of real and simulated data, in detector operations, and in the trigger and data acquisition systems of the experiment.

3 Analysis

3.1 Data and simulated event samples

This analysis uses pp collision data at a centre-of-mass energy of $\sqrt{s} = 13$ TeV collected by the ATLAS detector during the second data-taking run of the LHC, which took place between 2015 and 2018. After applying standard data-quality requirements for LHC and detector operations [25], this dataset corresponds to a total integrated luminosity of 139 fb^{-1} with an uncertainty of 1.7% [26], obtained using the LUCID-2 sub-detector [27] for the primary luminosity measurements. Candidate events were selected by a trigger that

¹ ATLAS uses a right-handed coordinate system with its origin at the nominal interaction point (IP) in the centre of the detector and the z -axis along the beam pipe. The x -axis points from the IP to the centre of the LHC ring, and the y -axis points upward. Cylindrical coordinates (r, ϕ) are used in the transverse plane, ϕ being the azimuthal angle around the z -axis. The pseudorapidity is defined in terms of the polar angle θ as $\eta = -\ln \tan(\theta/2)$.

required at least one electron–muon pair [28, 29]. The trigger-level thresholds for the p_T of the leptons were 17 GeV for the electron and 14 GeV for the muon. The thresholds applied in the lepton offline selection ensured that trigger efficiencies are constant in the relevant phase space.

Simulated MC event samples are used for the SM background estimates and to correct the signal distributions for detector effects. These were processed through a full simulation of the ATLAS detector [30] based on GEANT4 [31] and reconstructed with the same algorithms as those used for the data. The generation of the simulated event samples includes the effect of multiple pp interactions per bunch crossing (pile-up), as well as changes in detector response because of interactions in bunch crossings before or after the one containing the hard interaction. Differences between data and simulation in the lepton reconstruction efficiency, energy scale, energy resolution and trigger efficiency [32, 33], and in the b -tagging efficiency [34], are treated through correction factors that are derived from data and applied as weights to the simulated events. The MC samples are also reweighted so that the distribution of the average number of interactions per bunch crossing reproduces the observed distribution in the data.

Simulated WW signal samples were produced by summing $q\bar{q}$ - and gg -initiated samples. The $q\bar{q}$ -initiated WW signal was simulated at next-to-leading-order (NLO) accuracy in QCD using the POWHEG BOX v2 [35–37] generator interfaced to PYTHIA 8.186 [38] for the modelling of the parton shower, hadronisation, and underlying event, with parameter values set according to the AZNLO tune [39]. The CT10NLO parton distribution function (PDF) set [40] was used for the hard-scattering processes, whereas the CTEQ6L1 PDF set [41] was used for the parton shower [42]. The events were normalised to the cross-section calculated to next-to-next-to-leading order (NNLO) in QCD [43]. Loop-induced $gg \rightarrow WW \rightarrow \ell\nu\ell\nu$ events were simulated at LO with up to one additional parton emission using SHERPA 2.2.2, with virtual QCD corrections provided by the OPEN LOOPS library [42, 44–46]. The $gg \rightarrow WW$ process was normalised to its inclusive NLO QCD cross-section [47]. An alternative sample of $q\bar{q} \rightarrow WW$ events was simulated using SHERPA 2.2.2 [42, 48] with matrix elements at NLO accuracy in QCD for up to one additional parton emission and at LO accuracy for up to three additional parton emissions. For the SHERPA $q\bar{q}$ - and gg -initiated samples the NNPDF3.0NNLO set of PDFs was used [49], along with the dedicated set of tuned parton-shower parameters developed by the SHERPA authors. No alternative simulation is considered for the $gg \rightarrow WW$ process, which contributes only a small fraction of the signal.

Table 1 summarises the generators used for the SM backgrounds along with the relevant PDF sets, the set of tuned parameters used to configure the hadronisation and underly-

Table 1 Simulated background event samples with the corresponding matrix element and parton shower (PS) generators, cross-section order in α_s used to normalise the event yield, underlying-event tune and the generator PDF sets used. Where used, the label ‘V’ refers to a W or Z boson

Physics process	Generator	Parton shower	Normalisation	Tune	PDF (generator)	PDF (PS)
$t\bar{t}$	POWHEG BOX v2 [36, 37, 53, 54]	PYTHIA 8.230 [55]	NNLO+NNLL [56]	A14 [57]	NNPDF3.0NLO [49]	NNPDF2.3LO [58]
Single top (Wt)	POWHEG BOX v2 [36, 37, 59]	PYTHIA 8.230	NLO+NNLL [60, 61]	A14	NNPDF3.0NLO [49]	NNPDF2.3LO
$VZ = WZ, ZZ$	POWHEG BOX v2 [36, 37, 62, 63]	PYTHIA 8.210	NLO [42, 62, 63]	AZNLO [39]	CT10NLO [40]	CTEQ6L1 [64]
‘Others’:						
Higgs	POWHEG BOX v2 [35–37]	PYTHIA 8.212 [55]	NNLO+NNLL [65–71]	AZNLO [39]	PDF4LHC15NNLO [72]	CTEQ6L1
VVV	SHERPA 2.2.2 [42, 48, 73]	SHERPA 2.2.2	NLO [42, 48]	SHERPA default [42]	NNPDF3.0NNLO [49]	NNPDF3.0NNLO
$t\bar{t} + H$	MADGRAPH5_AMC@NLO [74]	PYTHIA 8.230 [55]	NLO [65]	A14	NNPDF3.0NLO	NNPDF2.3LO
$t\bar{t} + V$	MADGRAPH5_AMC@NLO	PYTHIA 8.210 [55]	NLO [74, 75]	A14	NNPDF3.0NLO	NNPDF2.3LO
$t\bar{t} + WW$	MADGRAPH5_AMC@NLO	PYTHIA 8.186 [38]	NLO [74]	A14	NNPDF2.3LO	NNPDF2.3LO
$tZ, t\bar{t}\bar{t}, t\bar{t}t$	MADGRAPH5_AMC@NLO	PYTHIA 8.230	NLO [74]	A14	NNPDF3.0NLO	NNPDF2.3LO
$Z/\gamma(\rightarrow \ell\ell)+jets$	SHERPA 2.2.1 [48, 73, 76]	SHERPA 2.2.1	NNLO [77]	SHERPA default [76]	NNPDF3.0NNLO	NNPDF3.0NNLO

ing event, and the cross-section order in α_s used to normalise the event yields for these samples. This study uses the same simulated samples and groupings for the SM background processes as the EWK $2\ell+0$ -jets search [22]. The ‘Others’ category groups together processes that produce small or negligible contributions to the signal regions of the search, and includes Drell–Yan, $t\bar{t}+V$ and Higgs boson production. Further information about the simulations of $t\bar{t}$, single-top (Wt), multiboson and boson-plus-jet processes can also be found in the relevant public ATLAS notes [42,50–52].

3.2 Event reconstruction and selection

Events are required to have at least one reconstructed vertex with at least two associated tracks with $p_T > 400$ MeV. When more than one vertex is reconstructed, the one with the highest $\sum p_T^2$ of associated tracks is taken to be the primary vertex. All final-state objects (electrons, muons and jets in this study) are required to satisfy ‘baseline’ criteria to ensure they are well-reconstructed and originate from the primary vertex, and additional ‘signal’ criteria are applied to define the objects used in the measurement. Baseline electrons are required to have $p_T > 10$ GeV, pseudorapidity $|\eta| < 2.47$ and a longitudinal impact parameter z_0 , relative to the primary vertex, satisfying $|z_0 \sin \theta| < 0.5$ mm; baseline muons must fulfill the same criteria except $|\eta| < 2.6$. Electrons must satisfy a *Loose* likelihood-based identification requirement [32], while muons must satisfy the *Medium* identification requirements defined in Ref. [33]. Signal electrons are required to satisfy a *Tight* identification requirement [32] and the track associated with the signal electron is required to have $|d_0|/\sigma(d_0) < 5$, where d_0 is the transverse impact parameter relative to the primary vertex and $\sigma(d_0)$ is its uncertainty, whilst for signal muons the associated track must have $|d_0|/\sigma(d_0) < 3$. The signal-lepton isolation criteria used in the EWK $2\ell+0$ -jets search [22] are also applied in this study. Hadronic jets are reconstructed from energy deposits in topological clusters of calorimeter cells [78,79] using the anti- k_r algorithm [80], as implemented in the Fast-Jet package [81], with a radius parameter $R = 0.4$. They are then calibrated by the application of a jet energy scale derived from 13 TeV data and simulation [82]. To reduce the effects of pile-up, for jets with $|\eta| < 2.5$ and $p_T < 120$ GeV a significant fraction of the tracks associated with each jet must have an origin compatible with the primary vertex, as defined by the jet vertex tagger [83]. For jets with $|\eta| > 2.5$ and $p_T < 60$ GeV, similar pile-up suppression is achieved through the forward jet vertex tagger [84]. Finally, events are rejected if they contain a jet that does not satisfy the jet-quality requirements [85,86]; this removes events impacted by detector noise or non-collision backgrounds. Jets containing b -hadrons (b -jets) are identified by the MV2c10 boosted decision tree algorithm [34], using quantities such

as the impact parameters of associated tracks along with well-reconstructed secondary vertices. A selection that provides 85% efficiency for tagging b -jets in simulated $t\bar{t}$ events is used in this study. Only jet candidates with $p_T > 20$ GeV and $|\eta| < 2.4$ are considered,² although all jets with $|\eta| < 4.9$ are included in the calculation of missing transverse momentum and in the procedure to remove reconstruction ambiguities that could lead to double counting of baseline objects. This procedure is applied as follows:

- jet candidates within $\Delta R' = \sqrt{(\Delta y)^2 + (\Delta\phi)^2} = 0.2$ of an electron candidate are removed;
- jets with fewer than three tracks that lie within $\Delta R' = 0.4$ of a muon candidate are removed;
- electrons and muons within $\Delta R' = 0.4$ of the remaining jets are discarded, to reject leptons from the decay of b - or c -hadrons;
- electron candidates are rejected if they are found to share an inner-detector track with a muon.

The measurements are performed in events with exactly one signal electron and one signal muon with opposite electric charge and each satisfying $p_T > 25$ GeV, and a veto on additional baseline leptons and hadronic jets. The multiplicities of non- b -tagged jets and b -tagged jets are considered separately in the background estimation for this study: events with exactly one b -tagged jet with a veto on additional non- b -tagged jets are used to estimate and validate the top-quark background. Requirements are also placed on the missing transverse momentum ($\mathbf{p}_T^{\text{miss}}$), which has magnitude E_T^{miss} . This is defined as the negative vector sum of the transverse momenta of all identified physics objects (electrons, photons, muons and jets), plus an additional ‘soft term’ to include low-momentum tracks associated with the primary vertex but not with these physics objects. The E_T^{miss} value is adjusted for the calibration of the selected physics objects [87].

To access a region of phase space similar to the WW control region in the EWK $2\ell+0$ -jets search, additional requirements are placed on the following variables in this study:

- The invariant mass of the dilepton system, $m_{e\mu} > 100$ GeV.
- The magnitude of the missing transverse momentum vector, $E_T^{\text{miss}} \in [60, 80]$ GeV.
- The ‘stransverse mass’ variable, $m_{T2} \in [60, 80]$ GeV [88, 89], with m_{T2} defined as:

$$m_{T2}(\mathbf{p}_{T,1}, \mathbf{p}_{T,2}, \mathbf{p}_T^{\text{miss}}) = \min_{\mathbf{q}_{T,1} + \mathbf{q}_{T,2} = \mathbf{p}_T^{\text{miss}}} \{ \max[m_T(\mathbf{p}_{T,1}, \mathbf{q}_{T,1}), m_T(\mathbf{p}_{T,2}, \mathbf{q}_{T,2})] \},$$

² Hadronic τ -lepton decay products are treated as jets.

Table 2 Summary of the selection criteria used for the signal region in this study. The same selections are used at detector level and particle level

Selection requirement	Criteria
Lepton flavour	$e^\pm \mu^\mp$
Lepton p_T	> 25 GeV
Lepton $ \eta $	< 2.47 (e^\pm), < 2.6 (μ^\mp)
Lepton veto	No additional electrons with $p_T > 10$ GeV, $ \eta < 2.47$ No additional muons with $p_T > 10$ GeV, $ \eta < 2.6$
$m_{e\mu}$	> 100 GeV
Jet veto	No jets with $p_T > 20$ GeV, $ \eta < 2.4$
m_{T2}	$\in [60, 80]$ GeV
E_T^{miss}	$\in [60, 80]$ GeV

where m_T is the transverse mass defined as $m_T = \sqrt{2 \times |\mathbf{p}_{T,a}| \times |\mathbf{p}_{T,b}| \times (1 - \cos(\Delta\phi))}$, and $\Delta\phi$ is the azimuthal angle between the particles with transverse momenta $\mathbf{p}_{T,a}$ and $\mathbf{p}_{T,b}$. The vectors $\mathbf{p}_{T,1}$ and $\mathbf{p}_{T,2}$ are the transverse momenta of the two leptons, and $\mathbf{q}_{T,1}$ and $\mathbf{q}_{T,2}$ satisfy $\mathbf{p}_T^{\text{miss}} = \mathbf{q}_{T,1} + \mathbf{q}_{T,2}$. The m_{T2} variable was designed to be sensitive to the mass scales of pair-produced heavy particles that each decay semi-invisibly. The minimisation is performed over all the possible decompositions of $\mathbf{p}_T^{\text{miss}}$ into two hypothetical invisible particles with momenta $\mathbf{q}_{T,1}$ and $\mathbf{q}_{T,2}$. For $t\bar{t}$ or WW decays, assuming an ideal detector with perfect momentum resolution, $m_{T2}(\mathbf{p}_{T,\ell_1}, \mathbf{p}_{T,\ell_2}, \mathbf{p}_T^{\text{miss}})$ has a kinematic endpoint at the mass of the W boson [89]. The signal regions of the EWK $2\ell+0$ -jets search required higher values, $m_{T2} > 100$ GeV.

In the EWK $2\ell+0$ -jets search, the top-quark contamination in events with a jet veto was observed to increase with m_{T2} in the region $m_{T2} \in [60, 100]$ GeV. To maximise WW purity, the control region required $m_{T2} \in [60, 65]$ GeV and $E_T^{\text{miss}} \in [60, 100]$ GeV with validation of the estimate being performed in events with $m_{T2} \in [65, 100]$ GeV and $E_T^{\text{miss}} > 60$ GeV. Since m_{T2} is sensitive to the angular separation of the lepton pair, the m_{T2} range is widened for the analysis described in this paper to provide a broader phase space for measuring angular distributions. Since E_T^{miss} and m_{T2} are correlated, the E_T^{miss} range is tightened to reduce the top-quark contamination. These changes increase the number of events in the region used to perform the differential cross-section measurements without reducing the WW purity. The previously used requirement on the ‘object-based E_T^{miss} significance’ [90] is removed to simplify the definition of the

fiducial region at particle level.³ The definition of the signal region used for this measurement is summarised in Table 2. The same selections are used at particle level when defining the fiducial region used for the fiducial and differential cross-section calculations, as discussed in Sect. 3.4.

Figure 1 shows detector-level comparisons between the data and the SM processes for the six variables that are unfolded to particle level in this study.

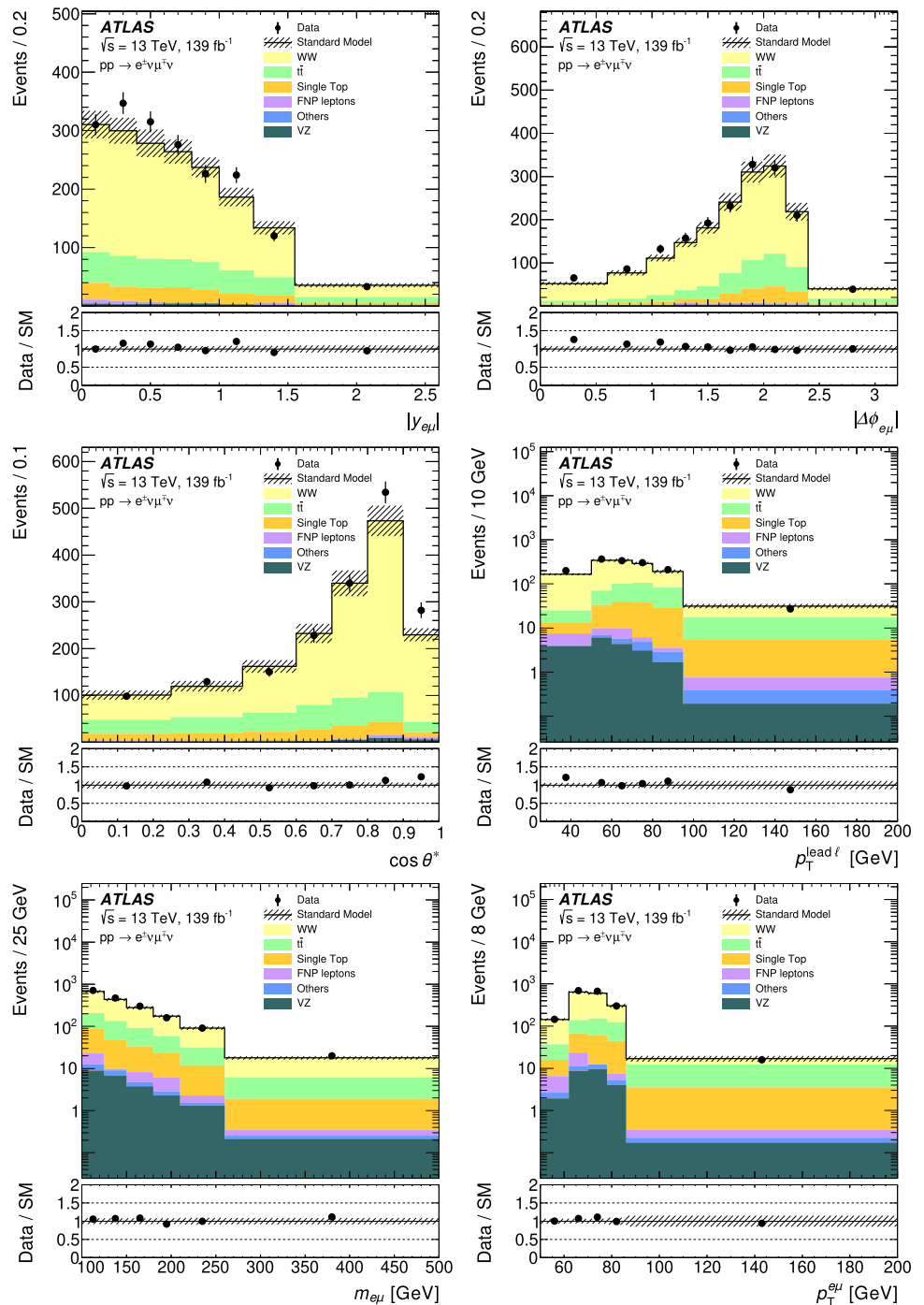
3.3 Background estimation

The estimation of the SM backgrounds in this study uses the same techniques as those used in the EWK $2\ell+0$ -jets search [22]. For the search, the SM backgrounds were classified into irreducible backgrounds from processes producing prompt leptons and reducible backgrounds containing one or more fake/non-prompt (FNP) leptons. The main irreducible backgrounds were SM diboson (WW , WZ , ZZ) and top-quark ($t\bar{t}$ and Wt) production, which were estimated from simulated events and normalised using a simultaneous likelihood fit to data in dedicated control regions (CRs). The yields and shapes of kinematic distributions of the relevant backgrounds were then validated in a set of validation regions (VRs). Three CRs were used: CR- WW , targeting WW production; CR-VZ, targeting WZ and ZZ production, which were normalised by using a single parameter in the likelihood fit to the data; and CR-top, targeting $t\bar{t}$ and single-top-quark production, which were also normalised by using a single parameter in the likelihood fit to the data. Both CR-VZ and CR-top require high m_{T2} , and high values of E_T^{miss} and its significance. CR-VZ uses same-flavour (dielectron and dimuon) events with a jet veto and requires the dilepton invariant mass to be consistent with an on-shell Z boson. CR-top requires one electron and one muon, one b -tagged jet with a veto on additional non- b -tagged jets. The remaining background from FNP leptons was estimated from data using the matrix method [91]. In this study, WW is the target signal process, with the remaining processes being backgrounds that are subtracted from the data prior to calculating the fiducial and differential cross-sections.

The statistical interpretation for the search was performed using the HistFitter framework [92]. The likelihood for the ‘background-only’ fit used to constrain the background normalisation factors was a product of Poisson probability density functions describing the observed number of events in

³ The ‘object-based E_T^{miss} significance’ helps to separate events with true E_T^{miss} (arising from weakly interacting particles) from those where it is consistent with particle mismeasurement, resolution effects or identification inefficiencies. On an event-by-event basis, given the full event composition, the E_T^{miss} significance evaluates the p -value that the observed E_T^{miss} is consistent with the null hypothesis of zero real E_T^{miss} , as further detailed in Ref. [90].

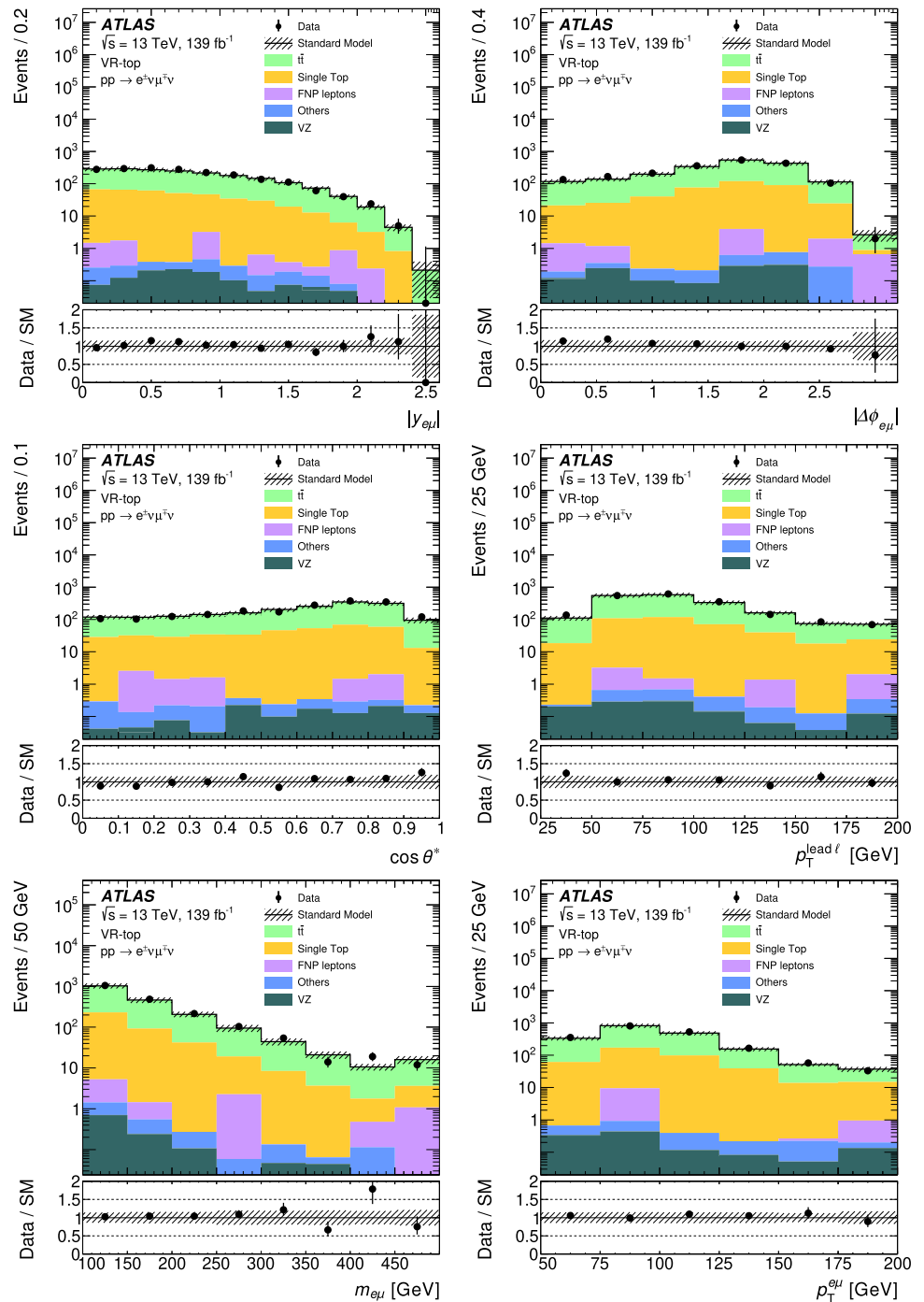
Fig. 1 Signal region detector-level distributions of $|y_{e\mu}|$ (top left), $|\Delta\phi_{e\mu}|$ (top right), $\cos\theta^*$ (middle left), $p_T^{\text{lead}\ell}$ (middle right), $m_{e\mu}$ (bottom left), and $p_T^{e\mu}$ (bottom right). Data are indicated by black markers along with the distribution for the WW signal and background SM processes. The last bin of each scale-variable distribution contains overflow events. The lower panels show the ratio of data to the total SM background prediction. The uncertainty bands shown include statistical and systematic uncertainties, excluding theory uncertainties in the WW signal. ‘FNP leptons’ refers to the background from fake/non-prompt leptons, calculated using the data-driven matrix method



each CR and Gaussian distributions that constrain the nuisance parameters associated with the systematic uncertainties. Poisson distributions were used for MC statistical uncertainties. Further details of the likelihood fit can be found in the EWK $2\ell+0$ -jets search paper [22]. After the fit, the normalisation factors returned for the WW , $t\bar{t}$ and single-top quark, and WZ/ZZ processes were 1.25 ± 0.11 , 0.82 ± 0.06 and 1.18 ± 0.05 respectively (where the errors include both statistical and systematic uncertainties), which for diboson

processes were applied to MC samples scaled to NLO QCD cross-sections (the NNLO QCD cross-sections were not used in the original search paper because the samples were normalised to the data in the control regions). Good agreement, within about one standard deviation, was observed for the yields and kinematic distributions in all VRs when applying these normalisation factors and their corresponding uncertainties. The deviation of the WW normalisation factor from unity by more than 1σ suggests there is tension between the

Fig. 2 Detector-level distributions of $|y_{e\mu}|$ (top left), $|\Delta\phi_{e\mu}|$ (top right), $\cos\theta^*$ (middle left), $p_T^{\text{lead } \ell}$ (middle right), $m_{e\mu}$ (bottom left), and $p_T^{e\mu}$ (bottom right) in the top validation region. Data are indicated by black markers along with the distribution for the WW signal and background SM processes. The last bin of each scale-variable distribution contains overflow events. The lower panels show the ratio of data to the total SM background prediction. The uncertainty bands shown include statistical and systematic uncertainties, excluding theory uncertainties in the WW signal. ‘FNP leptons’ refers to the background from fake/non-prompt leptons, calculated using the data-driven matrix method



SM and data in the parameter space probed by the search, and this is tested in the present study.

In this study, the normalisation factors from the EWK $2\ell+0$ -jets search are applied directly to the VZ (WZ/ZZ) and top ($t\bar{t}$, Wt) backgrounds that are subtracted from the data when performing the cross-section measurements described in Sect. 3.4. The uncertainties in the normalisation factors are propagated through the calculation as discussed in Sect. 3.5. The correlations and constraints that the likeli-

hood fit imposes on the nuisance parameters describing the systematic uncertainties are not applied in this study; the systematic uncertainties are instead assumed to take their nominal values as discussed in Sect. 3.5. This approach is designed to be conservative, but it has negligible impact on the results because no significant constraints were observed in the EWK $2\ell+0$ -jets search. To validate the use of the original top normalisation factor from the EWK $2\ell+0$ -jets search in the adjusted phase space of this study, an additional val-

idation exercise is performed to check the modelling of the top-quark background in a region with the same selection as in Table 2 but requiring exactly one b -tagged jet. Good agreement is observed across all six distributions considered for differential cross-section measurements, as shown in Fig. 2.

3.4 Fiducial cross-section determination

The differential cross-sections are measured in the fiducial phase space of the $WW \rightarrow e^\pm \nu \mu^\mp \nu$ decay channel using particle-level implementations of the selection criteria defined in Table 2. The particle-level quantities associated with simulated events are calculated using the SimpleAnalysis [93] framework. The signal particle-level distributions produced by SimpleAnalysis have been validated against the Rivet [94] toolkit that enables further reinterpretation of SM measurements and validation of MC generators. The Rivet routine for this measurement is available on HepData [95].

Electrons and muons are required to originate from the hard interaction and not from hadron decays. Electrons and muons from leptonically decaying τ -leptons are included in the fiducial region. The momenta of photons that are emitted in a cone of size $\Delta R' = 0.1$ around the lepton direction and do not originate from hadron decays are added to form ‘dressed’ leptons. Particle-level jets are reconstructed using the anti- k_t algorithm [80] with radius parameter $R = 0.4$ from visible stable final-state particles, excluding prompt dressed leptons. The particle-level missing transverse momentum is defined as the vectorial sum of the momenta of invisible particles in the event. For SM processes this is the sum of the neutrino momenta.

The fiducial cross-section is calculated as:

$$\sigma_{WW} = \frac{N_{\text{obs}} - N_{\text{bkg}}}{C \cdot \mathcal{L}},$$

where N_{obs} is the observed number of data events in the fiducial region, N_{bkg} is the predicted number of background events, \mathcal{L} the integrated luminosity, and C is a correction factor to account for limited acceptances and detector inefficiencies. It is calculated using MC simulation as the number of simulated signal events passing the detector-level event selection divided by the number of events in the fiducial phase space. In this study, $C = 0.55 \pm 0.08$ is applied, where the uncertainty comes from statistical, experimental and theoretical sources, as described in Sect. 3.5.

The differential cross-sections are calculated using the iterative Bayesian unfolding (IBU) technique [96,97] as implemented in the RooUnfold package [98]. This unfolding technique corrects the detector-level distributions of data (with the non- WW backgrounds subtracted) for bin-to-bin migrations due to the event reconstruction. It also applies fiducial corrections (corresponding to events that are recon-

structed in the signal region but originate outside the fiducial region at particle level) and reconstruction efficiency corrections (due to events that lie inside the fiducial region at particle level but do not enter the signal region due to detector inefficiencies). The bins chosen for the differential measurements were optimised for a desired level of statistical uncertainty and to reduce the migration of events between particle-level and detector-level bins. The number of iterations used in IBU is also optimised by considering the bias due to the assumed true distribution and the resulting statistical uncertainty of the measurement, with too many iterations generating high statistical uncertainties and too few iterations biasing the measurements towards the MC prediction. In this study, two iterations are chosen for $\cos \theta^*$ and $|\Delta \phi_{e\mu}|$, three iterations are used for $m_{e\mu}$ and $p_T^{\text{lead } \ell}$, and four iterations are used for $|y_{e\mu}|$ and $p_T^{e\mu}$. In addition to the bias tests (discussed in Sect. 3.5) to measure any systematic effects due to the use of the signal WW MC sample in the unfolding procedure, several signal injection tests were performed using SUSY models for chargino-pair production that were on the edge of the exclusion sensitivity in the EWK $2\ell+0$ -jets search. These are important checks of the validity of using these measurements to calculate constraints on BSM physics. Detector-level distributions of WW plus injected BSM signal were input to the unfolding calculation to test whether the particle-level WW plus BSM distribution could be recovered. The unfolding calculation matched the expected WW plus BSM distributions for a range of SUSY models displaying different kinematics because of their different SUSY particle masses. The results of the BSM injection tests are available on HepData [95].

3.5 Systematic uncertainties

Systematic uncertainties in the WW differential cross-sections measured in this study arise from experimental sources (which impact the subtracted non- WW backgrounds, and the calculation used to correct the signal for detector effects), uncertainties in the modelling of the top-quark background (which includes theoretical uncertainties, and uncertainties associated with the data-driven background estimate), and signal modelling. Statistical uncertainties associated with the MC samples used for the signal and background processes, and with the observed data distributions, also impact the unfolded distributions.

The sources of experimental uncertainty considered in the EWK $2\ell+0$ -jets search [22] are also considered in this study. The dominant experimental uncertainties are due to the calibration of the jet energy scale and resolution [79,82]. Additional uncertainties that arise from the lepton reconstruction efficiency, lepton energy scale and lepton energy resolution, and differences between the trigger efficiencies in data and simulation are grouped into the lepton uncertainties category. There are also uncertainties in the scale factors applied

to the simulated samples to account for differences between data and simulation in the b -jet identification efficiency, and an uncertainty in p_T^{miss} associated with the soft-term resolution and scale [87]. Finally, an uncertainty is assigned to the reweighting procedure (pile-up reweighting) applied to simulated events to match the distribution of the number of interactions per bunch crossing observed in data.

Several sources of uncertainty in the modelling of $t\bar{t}$ and Wt events are accounted for by varying the normalisation and shape of the subtracted backgrounds. For $t\bar{t}$ production, uncertainties in the parton shower simulation are estimated from differences between samples generated with POWHEG BOX interfaced to either PYTHIA8.186 or HERWIG 7.04 [99, 100]. Uncertainties in the modelling of initial- and final-state radiation are estimated by comparing the nominal sample with two alternative samples generated with POWHEG BOX interfaced to PYTHIA8.186 but with the radiation settings varied [101]. Finally, an additional uncertainty associated with the choice of event generator is estimated by comparing the nominal samples with samples generated with MADGRAPH5_AMC@NLO interfaced to PYTHIA 8.186 [102]. For single-top-quark production, an uncertainty is assigned to the treatment of the interference between the Wt and $t\bar{t}$ samples. This is done by comparing the nominal sample generated using the diagram removal method with a sample generated using the diagram subtraction method [101].

Of the systematic uncertainties considered in the EWK $2\ell+0$ -jets search, uncertainties in the data-driven estimate of FNP leptons and theoretical uncertainties in the diboson WZ/ZZ backgrounds are not applied in this study because these processes contribute little to the subtracted backgrounds. Additional systematic uncertainties are applied to the unfolding to account for the uncertainty in the normalisation of the top-quark and VZ backgrounds, although the VZ normalisation uncertainties are observed to be negligible. The luminosity uncertainty (1.7%) is applied to the subtracted backgrounds that are not estimated using data-driven techniques.

Tests were performed to estimate the bias introduced by using information from the nominal signal MC sample in the unfolding procedure. This includes a data-driven test, whereby MC simulated WW signal events are reweighted at generator level to obtain better agreement between the detector-level signal and the background-subtracted data. The nominal unfolding procedure is then applied to the reweighted detector-level signal distributions to check whether the reweighted particle-level distributions can be reproduced. The impact of theoretical uncertainties in the signal modelling is evaluated by using the detector-level signal distributions with the alternative SHERPA $qq \rightarrow WW$ signal sample introduced in Sect. 3.1 as input to the nominal unfolding procedure, and comparing the result with the

alternative particle-level signal distribution. In all tests the expected particle-level distributions were accurately recovered so no additional uncertainties were assigned to the unfolding procedure.

Finally, statistical uncertainties from the data are calculated using pseudo-experiments that vary the data distributions according to their Poisson uncertainties in each bin, which are then passed through the unfolding calculation. Statistical uncertainties associated with the simulated MC samples are evaluated using a similar technique.

4 Results

The measured fiducial cross-section for $WW \rightarrow e^\pm \nu \mu^\mp \nu$ production in the phase space defined in Table 2 is:

$$\begin{aligned} \sigma(WW \rightarrow e^\pm \nu \mu^\mp \nu) &= 19.2 \pm 0.3 \text{ (stat)} \pm 2.5 \text{ (syst)} \pm 0.4 \text{ (lumi)} \text{ fb} \\ &= 19.2 \pm 2.6 \text{ (total)} \text{ fb.} \end{aligned}$$

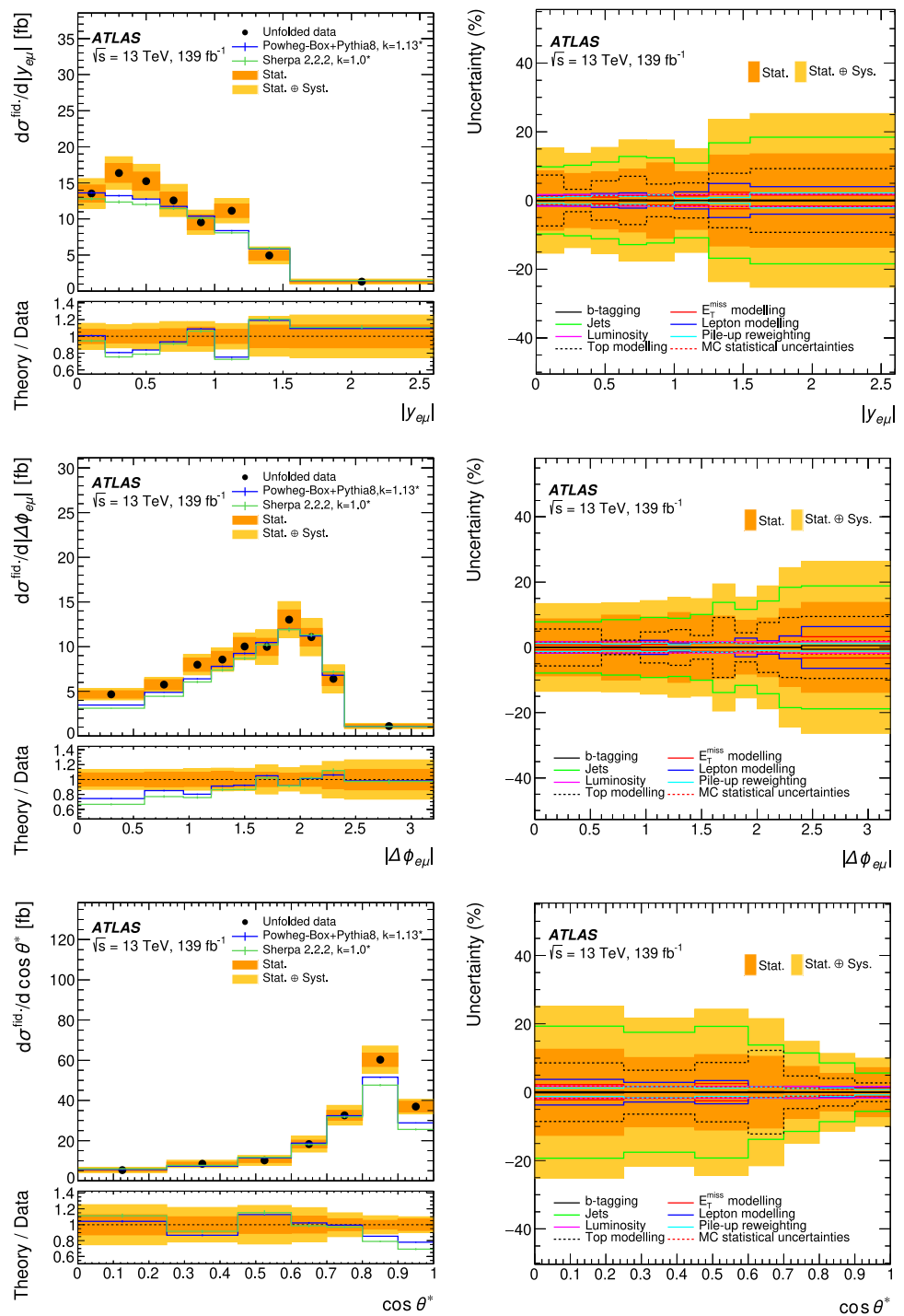
Table 3 shows the relative impact of the categories of systematic uncertainties discussed in Sect. 3.5 on the measured fiducial cross-section. The largest contribution is from the experimental jet uncertainty, which contributes a 12% uncertainty to the measured fiducial cross-section. The jet uncertainties are higher than in the previous ATLAS 13 TeV $WW+0$ -jet measurement [15] and this can be attributed to the lower p_T threshold used to define the jet veto.

The measured value is compatible with the nominal predictions of 17.8 fb and 17.1 fb from POWHEG BOX v2+PYTHIA 8.186 and SHERPA 2.2.2, respectively, where both are combined with SHERPA 2.2.2+OPEN LOOPS (LO+PS) for the gg -initiated states. The ratio of the measured cross-section to the nominal POWHEG BOX v2+PYTHIA 8.186 prediction is 1.08. To compare this ratio with the

Table 3 Breakdown of the relative uncertainties per category and the total uncertainty on the fiducial cross-section measurement

Uncertainty source	Uncertainty [%]
Jets	11.7
Top modelling	4.8
Data statistics	3.1
Lepton modelling	1.9
Luminosity	1.7
Pile-up reweighting	1.2
E_T^{miss} modelling	1.1
MC statistical uncertainties	0.5
Total systematic uncertainty	13.0
Total uncertainty	13.4

Fig. 3 Measured fiducial differential cross-sections of WW production for (top to bottom) $|y_{e\mu}|$, $|\Delta\phi(e\mu)|$ and $\cos\theta^*$. The measured cross-section values are shown as points with dark bands giving the statistical uncertainty and light bands indicating the size of the total uncertainty. The results are compared with the $q\bar{q}$ -initiated predictions from POWHEG BOX V2+PYTHIA 8.186 and SHERPA 2.2.2, each combined with SHERPA 2.2.2+OPEN LOOPS (LO+PS) for the gg -initiated states. The k -factors refer to the corrections applied to the predictions of $q\bar{q}$ -initiated and gg -initiated processes to NNLO and NLO accuracy in QCD respectively. The right column shows a breakdown of contributions to the uncertainties in the unfolded measurement



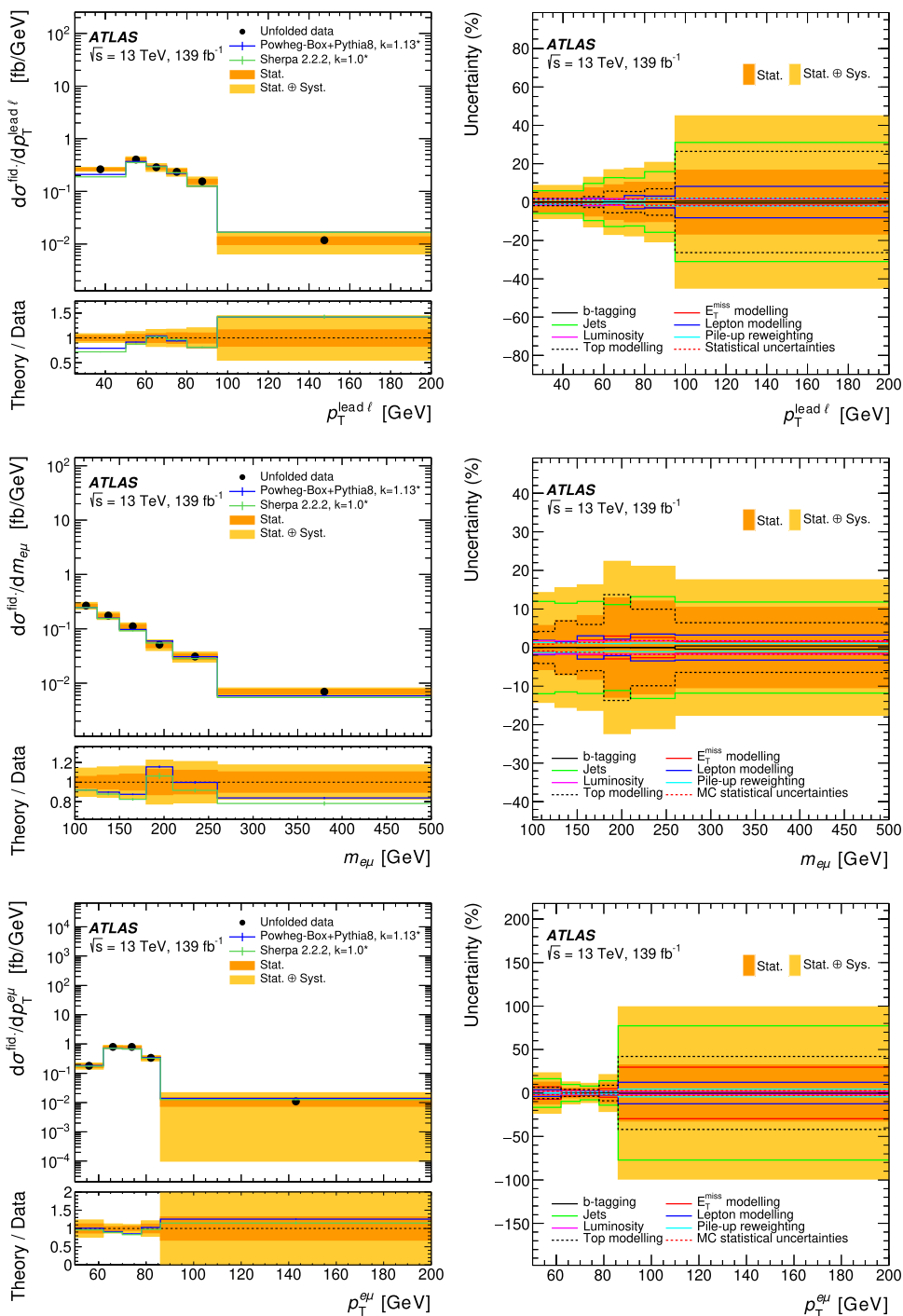
detector-level WW normalisation factor of 1.25 ± 0.11 in the EWK $2\ell+0$ -jets search [22], the former must be multiplied by 1.13 to account for the NLO cross-section calculation, which is included in this study but not in the EWK $2\ell+0$ -jets search. This gives a ratio of 1.22, which is consistent with the normalisation factor from the EWK $2\ell+0$ -jets search.

Particle-level differential cross-sections for the six variables targeted in this study are presented in Fig. 3 for the angular variables and Fig. 4 for the scale variables. In each

case, the right-hand plot shows the impact of the uncertainties, grouped into the categories discussed in Sect. 3.5, on the measurement.

The dilepton rapidity distribution has a maximum between $|y_{e\mu}| = 0$ and $|y_{e\mu}| = 1$, consistent with central production of a massive diboson system. The $|\Delta\phi_{e\mu}|$ distribution peaks at $|\Delta\phi_{e\mu}| = 2$. The shape of this distribution is influenced by the m_{T2} selection defining the fiducial region: high $|\Delta\phi_{e\mu}|$ values are associated with back-to-back leptons, which typi-

Fig. 4 Measured fiducial differential cross-sections of WW production for (top to bottom) $p_T^{\text{lead } \ell}$, $m_{e\mu}$ and $p_T^{e\mu}$. The last bin is inclusive in the measured observable and for $p_T^{e\mu}$ the first bin contains the underflow bin. The measured cross-section values are shown as points with dark bands giving the statistical uncertainty and light bands indicating the size of the total uncertainty. The results are compared with the $q\bar{q}$ -initiated predictions from POWHEG BOX V2+PYTHIA 8.186 and SHERPA 2.2.2, each combined with SHERPA 2.2.2+OPEN LOOPS (LO+PS) for the gg -initiated states. The k -factors refer to the corrections applied to scale the predictions of qq -initiated and gg -initiated processes to NNLO and NLO accuracy in QCD respectively. The right column shows a breakdown of contributions to the uncertainties in the unfolded measurement



cally give lower m_{T2} values than are considered in this study. Conversely, the highest m_{T2} values (which for WW production should occur around 90 GeV in the absence of detector effects) are often associated with collinear leptons (low $|\Delta\phi_{e\mu}|$), which are also excluded from the fiducial region. The $\cos\theta^*$ distribution peaks around $\cos\theta^* = 0.8$, with higher values being suppressed by the rapidity acceptance of the fiducial phase space. The distributions of the scale variables all show the expected characteristic fall for high values of the variable. The fiducial phase-space acceptance

also suppresses the leading-lepton and dilepton p_T distributions at lower p_T values.

The measurements are compared with the qq -initiated NLO QCD+PS predictions from POWHEG BOX v2+PYTHIA 8.186 and SHERPA 2.2.2, each combined with SHERPA 2.2.2+OPEN LOOPS (LO+PS) for the gg -initiated states. For the angular variables, the region with $|\Delta\phi_{e\mu}| < 1.5$ is underestimated by both theory predictions, which is consistent with observations in the previous ATLAS 13 TeV WW +0-jet measurement [15]. The region $\cos\theta^* > 0.8$ is

Table 4 Chi-squared per number of degrees of freedom χ^2/NDF for a comparison of unfolded distributions with different theory predictions. The calculation takes into account bin-by-bin correlations of systematic

and statistical uncertainties. Uncertainties in the theory predictions are not considered

	$ y_{e\mu} $	$ \Delta\phi_{e\mu} $	$\cos\theta^*$	$p_T^{\text{lead}\ell}$	$m_{e\mu}$	$p_T^{e\mu}$
POWHEG BOX v2+PYTHIA 8 ($q\bar{q}$) and SHERPA 2.2.2+OPEN LOOPS (gg)	14.4/8	10.1/10	13.3/7	15.4/6	2.8/6	3.9/5
SHERPA 2.2.2 ($q\bar{q}$) and SHERPA 2.2.2+OPEN LOOPS (gg)	18.3/8	17.9/10	24.5/7	24.1/6	2.5/6	4.1/5

also underestimated by 10–30% by both predictions. This corresponds to a rapidity difference of $|\Delta y(e\mu)| \geq 2.2$ between the leptons. For the distribution of dilepton rapidity $|y_{e\mu}|$, the theory shows reasonable agreement with the measurement. The predictions for the scale variables show good agreement with the data except for low values of $p_T^{\text{lead}\ell}$, where both predictions underestimate the cross-section by 20–25%. Global χ^2 calculations are carried out for all predictions and are displayed in Table 4. Uncertainties in the theory predictions are not considered. The largest χ^2/NDF is 24.1/6 corresponding to the comparison between the $q\bar{q} \rightarrow WW$ (SHERPA 2.2.2)+ $gg \rightarrow WW$ (SHERPA 2.2.2+OPEN LOOPS) prediction and the unfolded distribution for $p_T^{\text{lead}\ell}$.

5 Conclusion

The cross-section for $WW \rightarrow e^\pm\nu\mu^\mp\nu$ production in pp collisions at $\sqrt{s} = 13$ TeV is measured with the ATLAS detector at the LHC in a fiducial phase-space characterised by the absence of jets and additional leptons, the presence of a high dilepton invariant mass $m_{e\mu}$, and with values of E_T^{miss} and the stransverse mass m_{T2} motivated by the control regions used in supersymmetry searches [22]. The measured cross-section is $\sigma(WW \rightarrow e^\pm\nu\mu^\mp\nu) = 19.2 \pm 0.3$ (stat) ± 2.5 (syst) ± 0.4 (lumi) fb. Differential cross-sections for three variables sensitive to the energy scale of the event and three variables sensitive to the angular correlations of the leptonic decay products are compared with two theoretical SM predictions from perturbative QCD calculations. Good agreement is observed for most distributions within the uncertainties. The largest discrepancies occur at low values of $|\Delta\phi_{e\mu}| < 1.5$, high values of $\cos\theta^* > 0.8$ and low $p_T^{\text{lead}\ell}$, which is consistent with the observations of the previous ATLAS $WW+0$ -jet measurement [15]. This study validates the SM in a new and interesting region motivated particularly by searches for supersymmetry and provides benchmark measurements that can be used to improve future SM predictions and calculate additional constraints on BSM models.

Acknowledgements We thank CERN for the very successful operation of the LHC, as well as the support staff from our institutions without whom ATLAS could not be operated efficiently. We acknowledge the support of ANPCyT, Argentina; YerPhI, Armenia; ARC, Australia; BMWFW and FWF, Austria; ANAS, Azerbaijan; CNPq and FAPESP, Brazil; NSERC, NRC and CFI, Canada; CERN; ANID, Chile; CAS, MOST and NSFC, China; Minciencias, Colombia; MEYS CR, Czech Republic; DNRF and DNSRC, Denmark; IN2P3-CNRS and CEA-DRF/IRFU, France; SRNSFG, Georgia; BMBF, HGF and MPG, Germany; GSRI, Greece; RGC and Hong Kong SAR, China; ISF and Benozio Center, Israel; INFN, Italy; MEXT and JSPS, Japan; CNRST, Morocco; NWO, Netherlands; RCN, Norway; MEiN, Poland; FCT, Portugal; MNE/IFA, Romania; MESTD, Serbia; MSSR, Slovakia; ARRS and MIZŠ, Slovenia; DSI/NRF, South Africa; MICINN, Spain; SRC and Wallenberg Foundation, Sweden; SERI, SNSF and Cantons of Bern and Geneva, Switzerland; MOST, Taiwan; TENMAK, Türkiye; STFC, United Kingdom; DOE and NSF, United States of America. In addition, individual groups and members have received support from BCKDF, CANARIE, Compute Canada and CRC, Canada; PRIMUS 21/SCI/017 and UNCE SCI/013, Czech Republic; COST, ERC, ERDF, Horizon 2020 and Marie Skłodowska-Curie Actions, European Union; Investissements d’Avenir Labex, Investissements d’Avenir IDEX and ANR, France; DFG and AvH Foundation, Germany; Herakleitos, Thales and Aristeia programmes co-financed by EU-ESF and the Greek NSRF, Greece; BSF-NSF and MINERVA, Israel; Norwegian Financial Mechanism 2014–2021, Norway; NCN and NAWA, Poland; La Caixa Banking Foundation, CERCA Programme Generalitat de Catalunya and PROMETEO and GenT Programmes Generalitat Valenciana, Spain; Göran Gustafssons Stiftelse, Sweden; The Royal Society and Leverhulme Trust, United Kingdom. The crucial computing support from all WLCG partners is acknowledged gratefully, in particular from CERN, the ATLAS Tier-1 facilities at TRIUMF (Canada), NDGF (Denmark, Norway, Sweden), CC-IN2P3 (France), KIT/GridKA (Germany), INFN-CNAF (Italy), NL-T1 (Netherlands), PIC (Spain), ASGC (Taiwan), RAL (UK) and BNL (USA), the Tier-2 facilities worldwide and large non-WLCG resource providers. Major contributors of computing resources are listed in Ref. [103].

Data Availability Statement This manuscript has associated data in a data repository. [Authors’ comment: All ATLAS scientific output is published in journals, and preliminary results are made available in Conference Notes. All are openly available, without restriction on use by external parties beyond copyright law and the standard conditions agreed by CERN. Data associated with journal publications are also made available: tables and data from plots (e.g. cross section values, likelihood profiles, selection efficiencies, cross section limits, ...) are stored in appropriate repositories such as HEPDATA (<http://hepdata.cedar.ac.uk/>). ATLAS also strives to make additional material related to the paper available that allows a reinterpretation of the data in the context of new theoretical models. For example, an extended encapsulation of the analysis is often provided for measurements in the

framework of RIVET (<http://rivet.hepforge.org/>). This information is taken from the ATLAS Data Access Policy, which is a public document that can be downloaded from <http://opendata.cern.ch/record/413> [opendata.cern.ch]].

Open Access This article is licensed under a Creative Commons Attribution 4.0 International License, which permits use, sharing, adaptation, distribution and reproduction in any medium or format, as long as you give appropriate credit to the original author(s) and the source, provide a link to the Creative Commons licence, and indicate if changes were made. The images or other third party material in this article are included in the article's Creative Commons licence, unless indicated otherwise in a credit line to the material. If material is not included in the article's Creative Commons licence and your intended use is not permitted by statutory regulation or exceeds the permitted use, you will need to obtain permission directly from the copyright holder. To view a copy of this licence, visit <http://creativecommons.org/licenses/by/4.0/>.

Funded by SCOAP³. SCOAP³ supports the goals of the International Year of Basic Sciences for Sustainable Development.

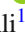
References

1. Y. Golfand, E. Likhtman, Extension of the algebra of Poincaré group generators and violation of P invariance. *JETP Lett.* **13**, 323 (1971). [*Pisma Zh. Eksp. Teor. Fiz.* **13**, 452 (1971)]
2. D. Volkov, V. Akulov, Is the neutrino a goldstone particle? *Phys. Lett. B* **46**, 109 (1973)
3. J. Wess, B. Zumino, Supergauge transformations in four dimensions. *Nucl. Phys. B* **70**, 39 (1974)
4. J. Wess, B. Zumino, Supergauge invariant extension of quantum electrodynamics. *Nucl. Phys. B* **78**, 1 (1974)
5. S. Ferrara, B. Zumino, Supergauge invariant Yang–Mills theories. *Nucl. Phys. B* **79**, 413 (1974)
6. A. Salam, J. Strathdee, Super-symmetry and non-Abelian gauges. *Phys. Lett. B* **51**, 353 (1974)
7. ATLAS Collaboration, The ATLAS experiment at the CERN large hadron collider. *JINST* **3**, S08003 (2008)
8. ATLAS Collaboration, Searches for scalar leptoquarks and differential cross-section measurements in dilepton-dijet events in proton–proton collisions at a centre-of-mass energy of $\sqrt{s} = 13$ TeV with the ATLAS experiment. *Eur. Phys. J. C* **79**, 733 (2019). [arXiv:1902.00377](https://arxiv.org/abs/1902.00377) [hep-ex]
9. ATLAS Collaboration, Measurement of W^+W^- production in pp collisions at $\sqrt{s} = 7$ TeV with the ATLAS detector and limits on anomalous WWZ and WW_γ couplings. *Phys. Rev. D* **87**, 112001 (2013). [arXiv:1210.2979](https://arxiv.org/abs/1210.2979) [hep-ex]. [Erratum: *Phys. Rev. D* **88**, 079906 (2013)]
10. CMS Collaboration, Measurement of the W^+W^- cross section in pp collisions at $\sqrt{s} = 8$ TeV and limits on anomalous WW_γ and WWZ couplings. *Eur. Phys. J. C* **73**, 2610 (2013). [arXiv:1306.1126](https://arxiv.org/abs/1306.1126) [hep-ex]
11. ATLAS Collaboration, Measurement of total and differential W^+W^- production cross sections in proton–proton collisions at $\sqrt{s} = 8$ TeV with the ATLAS detector and limits on anomalous triple-gauge-boson couplings. *JHEP* **09**, 029 (2016). [arXiv:1603.01702](https://arxiv.org/abs/1603.01702) [hep-ex]
12. CMS Collaboration, Measurement of the W^+W^- cross section in pp collisions at $\sqrt{s} = 8$ TeV and limits on anomalous gauge couplings. *Eur. Phys. J. C* **76**, 401 (2016). [arXiv:1507.03268](https://arxiv.org/abs/1507.03268) [hep-ex]
13. ATLAS Collaboration, Measurement of W^+W^- production in association with one jet in proton–proton collisions at $\sqrt{s} = 8$ TeV with the ATLAS detector. *Phys. Lett. B* **763**, 114 (2016). [arXiv:1608.03086](https://arxiv.org/abs/1608.03086) [hep-ex]
14. ATLAS Collaboration, Measurement of the W^+W^- production cross section in pp collisions at a centre-of-mass energy of $\sqrt{s} = 13$ TeV with the ATLAS experiment. *Phys. Lett. B* **773**, 354. [arXiv:1702.04519](https://arxiv.org/abs/1702.04519) [hep-ex]
15. ATLAS Collaboration, Measurement of fiducial and differential W^+W^- production cross-sections at $\sqrt{s} = 13$ TeV with the ATLAS detector. *Eur. Phys. J. C* **79**, 884 (2019). [arXiv:1905.04242](https://arxiv.org/abs/1905.04242) [hep-ex]
16. ATLAS Collaboration, Measurements of $W^+W^- + \geq 1$ jet production cross-sections in pp collisions at $\sqrt{s} = 13$ TeV with the ATLAS detector. *JHEP* **06**, 003 (2021). [arXiv:2103.10319](https://arxiv.org/abs/2103.10319) [hep-ex]
17. CMS Collaboration, W^+W^- boson pair production in proton–proton collisions at $\sqrt{s} = 13$ TeV. *Phys. Rev. D* **102**, 092001 (2020). [arXiv:2009.00119](https://arxiv.org/abs/2009.00119) [hep-ex]
18. ALEPH, DELPHI, L3 and OPAL Collaborations and the LEP Electroweak Working Group, Electroweak measurements in electron–positron collisions at W-boson-pair energies at LEP. *Phys. Rep.* **532**, 119 (2013). [arXiv:1302.3415](https://arxiv.org/abs/1302.3415) [hep-ex]
19. CDF Collaboration, Observation of W^+W^- production in $p\bar{p}$ collisions at $\sqrt{s} = 1.8$ TeV. *Phys. Rev. Lett.* **78**, 4536 (1997)
20. CDF Collaboration, Measurement of the W^+W^- production cross section and search for anomalous WW_γ and WWZ couplings in $p\bar{p}$ collisions at $\sqrt{s} = 1.96$ TeV. *Phys. Rev. Lett.* **104**, 201801 (2010). [arXiv:0912.4500](https://arxiv.org/abs/0912.4500) [hep-ex]. [Erratum: *Phys. Rev. Lett.* **104**, 201801 (2010)]
21. DØ Collaboration, Measurement of the WW production cross section with dilepton final states in $p\bar{p}$ collisions at $\sqrt{s} = 1.96$ TeV and limits on anomalous trilinear gauge couplings. *Phys. Rev. Lett.* **103**, 191801 (2009). [arXiv:0904.0673](https://arxiv.org/abs/0904.0673) [hep-ex]
22. ATLAS Collaboration, Search for electroweak production of charginos and sleptons decaying into final states with two leptons and missing transverse momentum in $\sqrt{s} = 13$ TeV pp collisions using the ATLAS detector. *Eur. Phys. J. C* **80**, 123 (2020). [arXiv:1908.08215](https://arxiv.org/abs/1908.08215) [hep-ex]
23. A.J. Barr, Measuring slepton spin at the LHC. *JHEP* **02**, 042 (2006). [arXiv:hep-ph/0511115](https://arxiv.org/abs/hep-ph/0511115)
24. ATLAS Collaboration, The ATLAS collaboration software and firmware. ATL-SOFT-PUB-2021-001 (2021). <https://cds.cern.ch/record/2767187>
25. ATLAS Collaboration, ATLAS data quality operations and performance for 2015–2018 data-taking. *JINST* **15**, P04003 (2020). [arXiv:1911.04632](https://arxiv.org/abs/1911.04632) [physics.ins-det]
26. ATLAS Collaboration, Luminosity determination in pp collisions at $\sqrt{s} = 13$ TeV using the ATLAS detector at the LHC. ATLAS-CONF-2019-021 (2019). <https://cds.cern.ch/record/2677054>
27. G. Avoni et al., The new LUCID-2 detector for luminosity measurement and monitoring in ATLAS. *JINST* **13**, P07017 (2018)
28. ATLAS Collaboration, Performance of electron and photon triggers in ATLAS during LHC Run 2. *Eur. Phys. J. C* **80**, 47 (2020). [arXiv:1909.00761](https://arxiv.org/abs/1909.00761) [hep-ex]
29. ATLAS Collaboration, Performance of the ATLAS muon triggers in Run 2. *JINST* **15**, P09015 (2020). [arXiv:2004.13447](https://arxiv.org/abs/2004.13447) [hep-ex]
30. ATLAS Collaboration, The ATLAS simulation infrastructure. *Eur. Phys. J. C* **70**, 823 (2010). [arXiv:1005.4568](https://arxiv.org/abs/1005.4568) [physics.ins-det]
31. GEANT4 Collaboration, S. Agostinelli et al., GEANT4—a simulation toolkit. *Nucl. Instrum. Methods A* **506**, 250 (2003)
32. ATLAS Collaboration, Electron and photon performance measurements with the ATLAS detector using the 2015–2017 LHC proton–proton collision data. *JINST* **14**, P12006 (2019). [arXiv:1908.00005](https://arxiv.org/abs/1908.00005) [hep-ex]
33. ATLAS Collaboration, Muon reconstruction performance of the ATLAS detector in proton–proton collision data at $\sqrt{s} = 13$ TeV. *Eur. Phys. J. C* **76**, 292 (2016). [arXiv:1603.05598](https://arxiv.org/abs/1603.05598) [hep-ex]
34. ATLAS Collaboration, ATLAS b -jet identification performance and efficiency measurement with $t\bar{t}$ events in pp collisions at

- $\sqrt{s} = 13$ TeV. Eur. Phys. J. C **79**, 970 (2019). [arXiv:1907.05120](https://arxiv.org/abs/1907.05120) [hep-ex]
35. P. Nason, A new method for combining NLO QCD with shower Monte Carlo algorithms. JHEP **11**, 040 (2004). [arXiv:hep-ph/0409146](https://arxiv.org/abs/hep-ph/0409146)
 36. S. Frixione, P. Nason, C. Oleari, Matching NLO QCD computations with parton shower simulations: the POWHEG method. JHEP **11**, 070 (2007). [arXiv:0709.2092](https://arxiv.org/abs/0709.2092) [hep-ph]
 37. S. Alioli, P. Nason, C. Oleari, E. Re, A general framework for implementing NLO calculations in shower Monte Carlo programs: the POWHEG BOX. JHEP **06**, 043 (2010). [arXiv:1002.2581](https://arxiv.org/abs/1002.2581) [hep-ph]
 38. T. Sjöstrand, S. Mrenna, P. Skands, A brief introduction to PYTHIA 8.1. Comput. Phys. Commun. **178**, 852 (2008). [arXiv:0710.3820](https://arxiv.org/abs/0710.3820) [hep-ph]
 39. ATLAS Collaboration, Measurement of the Z/γ^* boson transverse momentum distribution in pp collisions at $\sqrt{s} = 7$ TeV with the ATLAS detector. JHEP **09**, 145 (2014). [arXiv:1406.3660](https://arxiv.org/abs/1406.3660) [hep-ex]
 40. H.-L. Lai et al., New parton distributions for collider physics. Phys. Rev. D **82**, 074024 (2010). [arXiv:1007.2241](https://arxiv.org/abs/1007.2241) [hep-ph]
 41. J. Pumplin et al., New generation of parton distributions with uncertainties from global QCD analysis. JHEP **07**, 012 (2002). [arXiv:hep-ph/0201195](https://arxiv.org/abs/hep-ph/0201195)
 42. ATLAS Collaboration, Multi-boson simulation for 13 TeV ATLAS analyses. ATL-PHYS-PUB-2017-005 (2017). <https://cds.cern.ch/record/2261933>
 43. T. Gehrmann et al., W^+W^- production at hadron colliders in next to next to leading order QCD. Phys. Rev. Lett. **113**, 212001 (2014). [arXiv:1408.5243](https://arxiv.org/abs/1408.5243) [hep-ph]
 44. F. Buccioni et al., OpenLoops 2. Eur. Phys. J. C **79**, 866 (2019). [arXiv:1907.13071](https://arxiv.org/abs/1907.13071) [hep-ph]
 45. F. Cascioli, P. Maierhöfer, S. Pozzorini, Scattering amplitudes with open loops. Phys. Rev. Lett. **108**, 111601 (2012). [arXiv:1111.5206](https://arxiv.org/abs/1111.5206) [hep-ph]
 46. A. Denner, S. Dittmaier, L. Hofer, Collier: a Fortran-based complex one-loop library in extended regularizations. Comput. Phys. Commun. **212**, 220 (2017). [arXiv:1604.06792](https://arxiv.org/abs/1604.06792) [hep-ph]
 47. F. Caola, K. Melnikov, R. Röntsch, L. Tancredi, QCD corrections to W^+W^- production through gluon fusion. Phys. Lett. B **754**, 275 (2016). [arXiv:1511.08617](https://arxiv.org/abs/1511.08617) [hep-ph]
 48. E. Bothmann et al., Event generation with Sherpa 2.2. SciPost Phys. **7**, 034 (2019). [arXiv:1905.09127](https://arxiv.org/abs/1905.09127) [hep-ph]
 49. R.D. Ball et al., Parton distributions for the LHC run II. JHEP **04**, 040 (2015). [arXiv:1410.8849](https://arxiv.org/abs/1410.8849) [hep-ph]
 50. ATLAS Collaboration, Improvements in $t\bar{t}$ modelling using NLO+PS Monte Carlo generators for Run 2. ATL-PHYS-PUB-2018-009 (2018). <https://cds.cern.ch/record/2630327>
 51. ATLAS Collaboration, Simulation of top-quark production for the ATLAS experiment at $\sqrt{s} = 13$ TeV. ATL-PHYS-PUB-2016-004 (2016). <https://cds.cern.ch/record/2120417>
 52. ATLAS Collaboration, ATLAS simulation of boson plus jets processes in Run 2. ATL-PHYS-PUB-2017-006 (2017). <https://cds.cern.ch/record/2261937>
 53. S. Frixione, P. Nason, G. Ridolfi, A positive-weight next-to-leading-order Monte Carlo for heavy flavour hadroproduction. JHEP **09**, 126 (2007). [arXiv:0707.3088](https://arxiv.org/abs/0707.3088) [hep-ph]
 54. J.M. Campbell, R.K. Ellis, P. Nason, E. Re, Top-pair production and decay at NLO matched with parton showers. JHEP **04**, 114 (2015). [arXiv:1412.1828](https://arxiv.org/abs/1412.1828) [hep-ph]
 55. T. Sjöstrand et al., An introduction to PYTHIA 8.2. Comput. Phys. Commun. **191**, 159 (2015). [arXiv:1410.3012](https://arxiv.org/abs/1410.3012) [hep-ph]
 56. M. Czakon, A. Mitov, Top++: a program for the calculation of the top-pair cross-section at hadron colliders. Comput. Phys. Commun. **185**, 2930 (2014). [arXiv:1112.5675](https://arxiv.org/abs/1112.5675) [hep-ph]
 57. ATLAS Collaboration, ATLAS Pythia 8 tunes to 7 TeV data. ATL-PHYS-PUB-2014-021 (2014). <https://cds.cern.ch/record/1966419>
 58. R.D. Ball et al., Parton distributions with LHC data. Nucl. Phys. B **867**, 244 (2013). [arXiv:1207.1303](https://arxiv.org/abs/1207.1303) [hep-ph]
 59. E. Re, Single-top Wt -channel production matched with parton showers using the POWHEG method. Eur. Phys. J. C **71**, 1547 (2011). [arXiv:1009.2450](https://arxiv.org/abs/1009.2450) [hep-ph]
 60. M. Aliev et al., HATHOR-HAdronic Top and Heavy quarks cross section calculator. Comput. Phys. Commun. **182**, 1034 (2011). [arXiv:1007.1327](https://arxiv.org/abs/1007.1327) [hep-ph]
 61. P. Kant et al., HatHor for single top-quark production: updated predictions and uncertainty estimates for single top-quark production in hadronic collisions. Comput. Phys. Commun. **191**, 74 (2015). [arXiv:1406.4403](https://arxiv.org/abs/1406.4403) [hep-ph]
 62. T. Melia, P. Nason, R. Röntsch, G. Zanderighi, W^+W^- , WZ and ZZ production in the POWHEG BOX. JHEP **11**, 078 (2011). [arXiv:1107.5051](https://arxiv.org/abs/1107.5051) [hep-ph]
 63. P. Nason, G. Zanderighi, W^+W^- , WZ and ZZ production in the POWHEG-BOX-V2. Eur. Phys. J. C **74**, 2702 (2014). [arXiv:1311.1365](https://arxiv.org/abs/1311.1365) [hep-ph]
 64. J. Pumplin et al., New generation of parton distributions with uncertainties from global QCD analysis. JHEP **07**, 012 (2002). [arXiv:hep-ph/0201195](https://arxiv.org/abs/hep-ph/0201195)
 65. D. de Florian et al., Handbook of LHC Higgs cross sections: 4. Deciphering the nature of the Higgs sector (2016). [arXiv:1610.07922](https://arxiv.org/abs/1610.07922) [hep-ph]
 66. C. Anastasiou et al., High precision determination of the gluon fusion Higgs boson cross-section at the LHC. JHEP **05**, 058 (2016). [arXiv:1602.00695](https://arxiv.org/abs/1602.00695) [hep-ph]
 67. C. Anastasiou, C. Duhr, F. Dulat, F. Herzog, B. Mistlberger, Higgs boson gluon-fusion production in QCD at three loops. Phys. Rev. Lett. **114**, 212001 (2015). [arXiv:1503.06056](https://arxiv.org/abs/1503.06056) [hep-ph]
 68. F. Dulat, A. Lazopoulos, B. Mistlberger, iHiggs 2—inclusive Higgs cross sections. Comput. Phys. Commun. **233**, 243 (2018). [arXiv:1802.00827](https://arxiv.org/abs/1802.00827) [hep-ph]
 69. U. Aglietti, R. Bonciani, G. Degrossi, A. Vicini, Two-loop light fermion contribution to Higgs production and decays. Phys. Lett. B **595**, 432 (2004). [arXiv:hep-ph/0404071](https://arxiv.org/abs/hep-ph/0404071)
 70. S. Actis, G. Passarino, C. Sturm, S. Uccirati, NLO electroweak corrections to Higgs boson production at hadron colliders. Phys. Lett. B **670**, 12 (2008). [arXiv:0809.1301](https://arxiv.org/abs/0809.1301) [hep-ph]
 71. M. Bonetti, K. Melnikov, L. Tancredi, Higher order corrections to mixed QCD-EW contributions to Higgs boson production in gluon fusion. Phys. Rev. D **97**, 056017 (2018). [arXiv:1801.10403](https://arxiv.org/abs/1801.10403) [hep-ph]. [Erratum: Phys. Rev. D **97**, 099906 (2018)]
 72. J. Butterworth et al., PDF4LHC recommendations for LHC Run II. J. Phys. G **43**, 023001 (2016). [arXiv:1510.03865](https://arxiv.org/abs/1510.03865) [hep-ph]
 73. T. Gleisberg et al., Event generation with SHERPA 1.1. JHEP **02**, 007 (2009). [arXiv:0811.4622](https://arxiv.org/abs/0811.4622) [hep-ph]
 74. J. Alwall et al., The automated computation of tree-level and next-to-leading order differential cross sections, and their matching to parton shower simulations. JHEP **07**, 079 (2014). [arXiv:1405.0301](https://arxiv.org/abs/1405.0301) [hep-ph]
 75. ATLAS Collaboration, Modelling of the $t\bar{t}H$ and $t\bar{t}V$ ($V = W, Z$) processes for $\sqrt{s} = 13$ TeV ATLAS analyses. ATL-PHYS-PUB-2016-005 (2016). <https://cds.cern.ch/record/2120826>
 76. ATLAS Collaboration, Monte Carlo generators for the production of a W or Z/γ^* boson in association with jets at ATLAS in Run 2. ATL-PHYS-PUB-2016-003 (2016). <https://cds.cern.ch/record/2120133>
 77. R. Gavin, Y. Li, F. Petriello, S. Quackenbush, FEWZ 2.0: a code for hadronic Z production at next-to-next-to-leading order, Comput. Phys. Commun. **182**, 2388–2403 (2011). [arXiv:1011.3540](https://arxiv.org/abs/1011.3540) [hep-ph]

78. ATLAS Collaboration, Topological cell clustering in the ATLAS calorimeters and its performance in LHC Run 1. *Eur. Phys. J. C* **77**, 490 (2017). [arXiv:1603.02934](#) [hep-ex]
79. ATLAS Collaboration, Jet energy scale and resolution measured in proton–proton collisions at $\sqrt{s} = 13$ TeV with the ATLAS detector. *Eur. Phys. J. C* **81**, 689 (2020). [arXiv:2007.02645](#) [hep-ex]
80. M. Cacciari, G.P. Salam, G. Soyez, The anti- k_t jet clustering algorithm. *JHEP* **04**, 063 (2008). [arXiv:0802.1189](#) [hep-ph]
81. M. Cacciari, G.P. Salam, G. Soyez, FastJet user manual. *Eur. Phys. J. C* **72**, 1896 (2012). [arXiv:1111.6097](#) [hep-ph]
82. ATLAS Collaboration, Jet energy scale measurements and their systematic uncertainties in proton–proton collisions at $\sqrt{s} = 13$ TeV with the ATLAS detector. *Phys. Rev. D* **96**, 072002 (2017). [arXiv:1703.09665](#) [hep-ex]
83. ATLAS Collaboration, Tagging and suppression of pileup jets with the ATLAS detector. ATLAS-CONF-2014-018 (2014). <https://cds.cern.ch/record/1700870>
84. ATLAS Collaboration, Forward jet vertex tagging: a new technique for the identification and rejection of forward pileup jets. ATLAS-CONF-2015-034 (2015). <https://cds.cern.ch/record/2042098>
85. ATLAS Collaboration, Selection of jets produced in 13 TeV proton–proton collisions with the ATLAS detector. ATLAS-CONF-2015-029 (2015). <https://cds.cern.ch/record/2037702>
86. ATLAS Collaboration, Performance of pile-up mitigation techniques for jets in pp collisions at $\sqrt{s} = 8$ TeV using the ATLAS detector. *Eur. Phys. J. C* **76**, 581 (2016). [arXiv:1510.03823](#) [hep-ex]
87. ATLAS Collaboration, Performance of missing transverse momentum reconstruction with the ATLAS detector using proton–proton collisions at $\sqrt{s} = 13$ TeV. *Eur. Phys. J. C* **78**, 903 (2018). [arXiv:1802.08168](#) [hep-ex]
88. C.G. Lester, D.J. Summers, Measuring masses of semi-invisibly decaying particles pair produced at hadron colliders. *Phys. Lett. B* **463**, 99 (1999). [arXiv:hep-ph/9906349](#)
89. A. Barr, C. Lester, P. Stephens, $m(T_2)$: the truth behind the glamour. *J. Phys. G* **29**, 2343 (2003). [arXiv:hep-ph/0304226](#)
90. ATLAS Collaboration, Object-based missing transverse momentum significance in the ATLAS Detector. ATLAS-CONF-2018-038 (2018). <https://cds.cern.ch/record/2630948>
91. ATLAS Collaboration, Measurement of the top quark-pair production cross section with ATLAS in pp collisions at $\sqrt{s} = 7$ TeV. *Eur. Phys. J. C* **71**, 1577 (2011). [arXiv:1012.1792](#) [hep-ex]
92. M. Baak et al., HistFitter software framework for statistical data analysis. *Eur. Phys. J. C* **75**, 153 (2015). [arXiv:1410.1280](#) [hep-ex]
93. ATLAS Collaboration, SimpleAnalysis: truth-level analysis framework. ATLAS-PHYS-PUB-2022-017 (2022). <https://cds.cern.ch/record/2805991>
94. C. Bierlich et al., Robust independent validation of experiment and theory: rivet version 3. *SciPost Phys.* **8**, 026 (2020). [arXiv:1912.05451](#) [hep-ph]
95. E. Maguire, L. Heinrich, G. Watt, HEPData: a repository for high energy physics data. *J. Phys. Conf. Ser.* **898**, 102006 (2017), ed. by R. Mount, C. Tull. [arXiv:1704.05473](#) [hep-ex]
96. G. D’Agostini, A multidimensional unfolding method based on Bayes’ theorem. *Nucl. Instrum. Methods A* **362**, 487 (1995). ISSN:0168-9002
97. G. D’Agostini, Improved iterative Bayesian unfolding (2010). [arXiv:1010.0632](#) [physics.data-an]
98. T. Adye, Unfolding algorithms and tests using RooUnfold, in *Proceedings, 2011 Workshop on Statistical Issues Related to Discovery Claims in Search Experiments and Unfolding (PHYSTAT 2011)* (CERN, Geneva, 2011), p. 313. [arXiv:1105.1160](#) [physics.data-an]
99. M. Bähr et al., Herwig++ physics and manual. *Eur. Phys. J. C* **58**, 639 (2008). [arXiv:0803.0883](#) [hep-ph]
100. J. Bellm et al., Herwig 7.0/Herwig++ 3.0 release note. *Eur. Phys. J. C* **76**, 196 (2016). [arXiv:1512.01178](#) [hep-ph]
101. ATLAS Collaboration, Studies on top-quark Monte Carlo modelling for Top2016. ATLAS-CONF-2016-020 (2016). <https://cds.cern.ch/record/2216168>
102. ATLAS Collaboration, Studies on top-quark Monte Carlo modelling with Sherpa and MG5_aMC@NLO. ATLAS-CONF-2017-007 (2017). <https://cds.cern.ch/record/2261938>
103. ATLAS Collaboration, ATLAS computing acknowledgements. ATLAS-SOFT-PUB-2021-003 (2021). <https://cds.cern.ch/record/2776662>

ATLAS Collaboration*

G. Aad¹⁰¹ , B. Abbott¹¹⁹ , D. C. Abbott¹⁰² , K. Abeling⁵⁵ , S. H. Abidi²⁹ , A. Abouhorma^{35e} , H. Abramowicz¹⁵⁰ , H. Abreu¹⁴⁹ , Y. Abulaiti¹¹⁶ , A. C. Abusleme Hoffman^{136a} , B. S. Acharya^{68a,68b,o} , B. Achkar⁵⁵ , L. Adam⁹⁹ , C. Adam Bourdarios⁴ , L. Adamczyk^{84a} , L. Adamek¹⁵⁴ , S. V. Addepalli²⁶ , J. Adelman¹¹⁴ , A. Adiguzel^{21c} , S. Adorni⁵⁶ , T. Adye¹³³ , A. A. Affolder¹³⁵ , Y. Afik³⁶ , M. N. Agaras¹³ , J. Agarwala^{72a,72b} , A. Aggarwal⁹⁹ , C. Agheorghiesei^{27c} , J. A. Aguilar-Saavedra^{129f} , A. Ahmad³⁶ , F. Ahmadov^{38,w} , W. S. Ahmed¹⁰³ , X. Ai⁴⁸ , G. Aielli^{75a,75b} , I. Aizenberg¹⁶⁷ , M. Akbiyik⁹⁹ , T. P. A. Åkesson⁹⁷ , A. V. Akimov³⁷ , K. Al Khoury⁴¹ , G. L. Alberghi^{23b} , J. Albert¹⁶³ , P. Albicocco⁵³ , M. J. Alconada Verzini⁸⁹ , S. Alderweireldt⁵² , M. Aleksa³⁶ , I. N. Aleksandrov³⁸ , C. Alexa^{27b} , T. Alexopoulos¹⁰ , A. Alfonsi¹¹³ , F. Alfonsi^{23b} , M. Alhroob¹¹⁹ , B. Ali¹³¹ , S. Ali¹⁴⁷ , M. Aliev³⁷ , G. Alimonti^{70a} , C. Allaire³⁶ , B. M. M. Allbrooke¹⁴⁵ , P. P. Allport²⁰ , A. Aloisio^{71a,71b} , F. Alonso⁸⁹ , C. Alpigiani¹³⁷ , E. Alunno Camelia^{75a,75b} , M. Alvarez Estevez⁹⁸ , M. G. Alvigi^{71a,71b} , Y. Amaral Coutinho^{81b} , A. Ambler¹⁰³ , C. Amelung³⁶ , C. G. Ames¹⁰⁸ , D. Amidei¹⁰⁵ , S. P. Amor Dos Santos^{129a} , S. Amoroso⁴⁸ , K. R. Amos¹⁶¹ , C. S. Amrouche⁵⁶ , V. Ananiev¹²⁴ , C. Anastopoulos¹³⁸ , N. Andari¹³⁴ , T. Andeen¹¹ , J. K. Anders¹⁹ , S. Y. Andreev^{47a,47b} , A. Andreazza^{70a,70b} , S. Angelidakis⁹ , A. Angerami^{41,y} , A. V. Anisenkov³⁷ , A. Annovi^{73a} , C. Antel⁵⁶ , M. T. Anthony¹³⁸ , E. Antipov¹²⁰ , M. Antonelli⁵³ , D. J. A. Antrim^{17a} , F. Anulli^{74a} , M. Aoki⁸² , J. A. Aparisi Pozo¹⁶¹ , M. A. Aparo¹⁴⁵ , L. Aperio Bella⁴⁸ 

C. Appelt¹⁸, N. Aranzabal³⁶, V. Araujo Ferraz^{81a}, C. Arcangeletti⁵³, A. T. H. Arce⁵¹, E. Arena⁹¹, J.-F. Arguin¹⁰⁷, S. Argyropoulos⁵⁴, J.-H. Arling⁴⁸, A. J. Armbruster³⁶, O. Arnaez¹⁵⁴, H. Arnold¹¹³, Z. P. Arrubarrena Tame¹⁰⁸, G. Artoni^{74a,74b}, H. Asada¹¹⁰, K. Asai¹¹⁷, S. Asai¹⁵², N. A. Asbah⁶¹, E. M. Asimakopoulou¹⁵⁹, J. Assahsah^{35d}, K. Assamagan²⁹, R. Astalos^{28a}, R. J. Atkin^{33a}, M. Atkinson¹⁶⁰, N. B. Atlay¹⁸, H. Atmani^{62b}, P. A. Atmasiddha¹⁰⁵, K. Augsten¹³¹, S. Auricchio^{71a,71b}, A. D. Aurio²⁰, V. A. Austrup¹⁶⁹, G. Avner¹⁴⁹, G. Avolio³⁶, K. Axiotis⁵⁶, M. K. Ayoub^{14c}, G. Azuelos^{107.ac}, D. Babal^{28a}, H. Bachacou¹³⁴, K. Bachas^{151.q}, A. Bachiu³⁴, F. Backman^{47a,47b}, A. Badea⁶¹, P. Bagnaia^{74a,74b}, M. Bahmani¹⁸, A. J. Bailey¹⁶¹, V. R. Bailey¹⁶⁰, J. T. Baines¹³³, C. Bakalis¹⁰, O. K. Baker¹⁷⁰, P. J. Bakker¹¹³, E. Bakos¹⁵, D. Bakshi Gupta⁸, S. Balaji¹⁴⁶, R. Balasubramanian¹¹³, E. M. Baldin³⁷, P. Balek¹³², E. Ballabene^{70a,70b}, F. Balli¹³⁴, L. M. Baltes^{63a}, W. K. Balunas³², J. Balz⁹⁹, E. Banas⁸⁵, M. Bandieramonte¹²⁸, A. Bandyopadhyay²⁴, S. Bansal²⁴, L. Barak¹⁵⁰, E. L. Barberio¹⁰⁴, D. Barberis^{57a,57b}, M. Barbero¹⁰¹, G. Barbour⁹⁵, K. N. Barends^{33a}, T. Barillari¹⁰⁹, M.-S. Barisits³⁶, J. Barkeloo¹²², T. Barklow¹⁴², R. M. Barnett^{17a}, P. Baron¹²¹, D. A. Baron Moreno¹⁰⁰, A. Baroncelli^{62a}, G. Barone²⁹, A. J. Barr¹²⁵, L. Barranco Navarro^{47a,47b}, F. Barreiro⁹⁸, J. Barreiro Guimarães da Costa^{14a}, U. Barron¹⁵⁰, M. G. Barros Teixeira^{129a}, S. Barsov³⁷, F. Bartels^{63a}, R. Bartoldus¹⁴², A. E. Barton⁹⁰, P. Bartos^{28a}, A. Basalae⁴⁸, A. Basan⁹⁹, M. Baselga⁴⁹, I. Bashta^{76a,76b}, A. Bassalat^{66.z}, M. J. Basso¹⁵⁴, C. R. Basson¹⁰⁰, R. L. Bates⁵⁹, S. Batlamous^{35c}, J. R. Batley³², B. Batool¹⁴⁰, M. Battaglia¹³⁵, M. Bauce^{74a,74b}, P. Bauer²⁴, A. Bayirli^{21a}, J. B. Beacham⁵¹, T. Beau¹²⁶, P. H. Beauchemin¹⁵⁷, F. Becherer⁵⁴, P. Bechtel²⁴, H. P. Beck^{19.p}, K. Becker¹⁶⁵, C. Becot⁴⁸, A. J. Beddall^{21d}, V. A. Bednyakov³⁸, C. P. Bee¹⁴⁴, L. J. Beemster¹⁵, T. A. Beermann³⁶, M. Begalli^{81b}, M. Begel²⁹, A. Behera¹⁴⁴, J. K. Behr⁴⁸, C. Beirao Da Cruz E Silva³⁶, J. F. Beirer^{36,55}, F. Beisiegel²⁴, M. Belfkir^{115b}, G. Bella¹⁵⁰, L. Bellagamba^{23b}, A. Bellerive³⁴, P. Bellos²⁰, K. Beloborodov³⁷, K. Belotskiy³⁷, N. L. Belyaev³⁷, D. Bencheekroun^{35a}, F. Bendebeba^{35a}, Y. Benhammou¹⁵⁰, D. P. Benjamin²⁹, M. Benoit²⁹, J. R. Bensinger²⁶, S. Bentvelsen¹¹³, L. Beresford³⁶, M. Beretta⁵³, D. Berge¹⁸, E. Bergeas Kuutmann¹⁵⁹, N. Berger⁴, B. Bergmann¹³¹, J. Beringer^{17a}, S. Berlendis⁷, G. Bernardi⁵, C. Bernius¹⁴², F. U. Bernlochner²⁴, T. Berry⁹⁴, P. Berta¹³², A. Berthold⁵⁰, I. A. Bertram⁹⁰, O. Bessidskaia Bylund¹⁶⁹, S. Bethke¹⁰⁹, A. Betti⁴⁴, A. J. Bevan⁹³, M. Bhamjee^{33c}, S. Bhatta¹⁴⁴, D. S. Bhattacharya¹⁶⁴, P. Bhattarai²⁶, V. S. Bhopatkar⁶, R. Bi¹²⁸, R. Bi^{29.af}, R. M. Bianchi¹²⁸, O. Biebel¹⁰⁸, R. Bielski¹²², N. V. Biesuz^{73a,73b}, M. Biglietti^{76a}, T. R. V. Billoud¹³¹, M. Bindi⁵⁵, A. Bingul^{21b}, C. Bini^{74a,74b}, S. Biondi^{23a,23b}, A. Biondini⁹¹, C. J. Birch-sykes¹⁰⁰, G. A. Bird^{20,133}, M. Birman¹⁶⁷, T. Bisanz³⁶, D. Biswas^{168.k}, A. Bitadze¹⁰⁰, K. Björke¹²⁴, I. Bloch⁴⁸, C. Blocker²⁶, A. Blue⁵⁹, U. Blumenschein⁹³, J. Blumenthal⁹⁹, G. J. Bobbink¹¹³, V. S. Bobrovnikov³⁷, M. Boehler⁵⁴, D. Bogavac³⁶, A. G. Bogdanchikov³⁷, C. Bohm^{47a}, V. Boisvert⁹⁴, P. Bokan⁴⁸, T. Bold^{84a}, M. Bomben⁵, M. Bona⁹³, M. Boonekamp¹³⁴, C. D. Booth⁹⁴, A. G. Borbély⁵⁹, H. M. Borecka-Bielska¹⁰⁷, L. S. Borgna⁹⁵, G. Borissov⁹⁰, D. Bortoletto¹²⁵, D. Boscherini^{23b}, M. Bosman¹³, J. D. Bossio Sola³⁶, K. Bouaouda^{35a}, J. Boudreau¹²⁸, E. V. Bouhova-Thacker⁹⁰, D. Boumediene⁴⁰, R. Bouquet⁵, A. Boveia¹¹⁸, J. Boyd³⁶, D. Boye²⁹, I. R. Boyko³⁸, J. Bracinik²⁰, N. Brahimi^{62c,62d}, G. Brandt¹⁶⁹, O. Brandt³², F. Braren⁴⁸, B. Brau¹⁰², J. E. Brau¹²², W. D. Breaden Madden⁵⁹, K. Brendlinger⁴⁸, R. Brenner¹⁶⁷, L. Brenner³⁶, R. Brenner¹⁵⁹, S. Bressler¹⁶⁷, B. Brickwedde⁹⁹, D. Britton⁵⁹, D. Britzger¹⁰⁹, I. Brock²⁴, G. Brooijmans⁴¹, W. K. Brooks^{136f}, E. Brost²⁹, P. A. Bruckman de Renstrom⁸⁵, B. Brüers⁴⁸, D. Bruncko^{28b,*}, A. Bruni^{23b}, G. Bruni^{23b}, M. Bruschi^{23b}, N. Bruscinò^{74a,74b}, L. Bryngemark¹⁴², T. Buanes¹⁶, Q. Buat¹³⁷, P. Buchholz¹⁴⁰, A. G. Buckley⁵⁹, I. A. Budagov^{38,*}, M. K. Bugge¹²⁴, O. Bulekov³⁷, B. A. Bullard⁶¹, S. Burdin⁹¹, C. D. Burgard⁴⁸, A. M. Burger⁴⁰, B. Burghgrave⁸, J. T. P. Burr³², C. D. Burton¹¹, J. C. Burzynski¹⁴¹, E. L. Busch⁴¹, V. Büscher⁹⁹, P. J. Bussey⁵⁹, J. M. Butler²⁵, C. M. Buttar⁵⁹, J. M. Butterworth⁹⁵, W. Buttinger¹³³, C. J. Buxo Vazquez¹⁰⁶, A. R. Buzykaev³⁷, G. Cabras^{23b}, S. Cabrera Urbán¹⁶¹, D. Caforio⁵⁸, H. Cai¹²⁸, Y. Cai^{14a,14d}, V. M. M. Cairo³⁶, O. Cakir^{3a}, N. Calace³⁶, P. Calafiura^{17a}, G. Calderini¹²⁶, P. Calfayan⁶⁷, G. Callea⁵⁹, L. P. Caloba^{81b}, D. Calvet⁴⁰, S. Calvet⁴⁰, T. P. Calvet¹⁰¹, M. Calvetti^{73a,73b}, R. Camacho Toro¹²⁶, S. Camarda³⁶, D. Camarero Muñoz⁹⁸, P. Camarri^{75a,75b}, M. T. Camerlingo^{76a,76b}, D. Cameron¹²⁴, C. Camincher¹⁶³, M. Campanelli⁹⁵, A. Camplani⁴², V. Canale^{71a,71b}, A. Canesse¹⁰³, M. Cano Bret⁷⁹, J. Cantero¹⁶¹, Y. Cao¹⁶⁰, F. Capocasa²⁶, M. Capua^{43a,43b}, A. Carbone^{70a,70b}, R. Cardarelli^{75a}, J. C. J. Cardenas⁸, F. Cardillo¹⁶¹, T. Carli³⁶, G. Carlino^{71a}, B. T. Carlson^{128.r}, E. M. Carlson^{155a,163}, L. Carminati^{70a,70b}, M. Carnesale^{74a,74b}, S. Caron¹¹², E. Carquin^{136f}, S. Carrá^{70a,70b}, G. Carratta^{23a,23b}, J. W. S. Carter¹⁵⁴, T. M. Carter⁵², M. P. Casado^{13.h}, A. F. Casha¹⁵⁴, E. G. Castiglia¹⁷⁰, F. L. Castillo^{63a}, L. Castillo Garcia¹³, V. Castillo Gimenez¹⁶¹, N. F. Castro^{129a,129e}, A. Catinaccio³⁶

J. R. Catmore¹²⁴, V. Cavaliere²⁹, N. Cavalli^{23a,23b}, V. Cavasinni^{73a,73b}, E. Celebi^{21a}, F. Celli¹²⁵, M. S. Centonze^{69a,69b}, K. Cerny¹²¹, A. S. Cerqueira^{81a}, A. Cerri¹⁴⁵, L. Cerrito^{75a,75b}, F. Cerutti^{17a}, A. Cervelli^{23b}, S. A. Cetin^{21d}, Z. Chadi^{35a}, D. Chakraborty¹¹⁴, M. Chala^{129f}, J. Chan¹⁶⁸, W. S. Chan¹¹³, W. Y. Chan¹⁵², J. D. Chapman³², B. Chargeishvili^{148b}, D. G. Charlton²⁰, T. P. Charman⁹³, M. Chatterjee¹⁹, S. Chekanov⁶, S. V. Chekulaev^{155a}, G. A. Chelkov^{38a}, A. Chen¹⁰⁵, B. Chen¹⁵⁰, B. Chen¹⁶³, C. Chen^{62a}, H. Chen^{14c}, H. Chen²⁹, J. Chen^{62c}, J. Chen²⁶, S. Chen¹⁵², S. J. Chen^{14c}, X. Chen^{62c}, X. Chen^{14b,ab}, Y. Chen^{62a}, C. L. Cheng¹⁶⁸, H. C. Cheng^{64a}, A. Cheplakov³⁸, E. Cheremushkina⁴⁸, E. Cherepanova¹¹³, R. Cherkaoui El Moursli^{35e}, E. Cheu⁷, K. Cheung⁶⁵, L. Chevalier¹³⁴, V. Chiarella⁵³, G. Chiarelli^{73a}, G. Chiodini^{69a}, A. S. Chisholm²⁰, A. Chitan^{27b}, Y. H. Chiu¹⁶³, M. V. Chizhov³⁸, K. Choi¹¹, A. R. Chomont^{74a,74b}, Y. Chou¹⁰², E. Y. S. Chow¹¹³, T. Chowdhury^{33g}, L. D. Christopher^{33g}, K. L. Chu^{64a}, M. C. Chu^{64a}, X. Chu^{14a,14d}, J. Chudoba¹³⁰, J. J. Chwastowski⁸⁵, D. Cieri¹⁰⁹, K. M. Ciesla^{84a}, V. Cindro⁹², A. Ciocio^{17a}, F. Ciotto^{71a,71b}, Z. H. Citron^{167.1}, M. Citterio^{70a}, D. A. Ciubotaru^{27b}, B. M. Ciungu¹⁵⁴, A. Clark⁵⁶, P. J. Clark⁵², J. M. Clavijo Columbie⁴⁸, S. E. Clawson¹⁰⁰, C. Clement^{47a,47b}, J. Clercx⁴⁸, L. Clissa^{23a,23b}, Y. Coadou¹⁰¹, M. Cobal^{68a,68c}, A. Coccaro^{57b}, R. F. Coelho Barrue^{129a}, R. Coelho Lopes De Sa¹⁰², S. Coelli^{70a}, H. Cohen¹⁵⁰, A. E. C. Coimbra^{70a,70b}, B. Cole⁴¹, J. Collot⁶⁰, P. Conde Muñio^{129a,129g}, S. H. Connell^{33c}, I. A. Connelly⁵⁹, E. I. Conroy¹²⁵, F. Conventi^{71a,ad}, H. G. Cooke²⁰, A. M. Cooper-Sarkar¹²⁵, F. Cormier¹⁶², L. D. Corpe³⁶, M. Corradi^{74a,74b}, E. E. Corrigan⁹⁷, F. Corriveau^{103.v}, A. Cortes-Gonzalez¹⁸, M. J. Costa¹⁶¹, F. Costanza⁴, D. Costanzo¹³⁸, B. M. Cote¹¹⁸, G. Cowan⁹⁴, J. W. Cowley³², K. Cranmer¹¹⁶, S. Crépé-Renaudin⁶⁰, F. Crescioli¹²⁶, M. Cristinziani¹⁴⁰, M. Cristoforetti^{77a,77b,c}, V. Croft¹⁵⁷, G. Crosetti^{43a,43b}, A. Cueto³⁶, T. Cuhadar Donszelmann¹⁵⁸, H. Cui^{14a,14d}, Z. Cui⁷, A. R. Cukierman¹⁴², W. R. Cunningham⁵⁹, F. Curcio^{43a,43b}, P. Czodrowski³⁶, M. M. Czurylo^{63b}, M. J. Da Cunha Sargedas De Sousa^{62a}, J. V. Da Fonseca Pinto^{81b}, C. Da Via¹⁰⁰, W. Dabrowski^{84a}, T. Dado⁴⁹, S. Dahbi^{33g}, T. Dai¹⁰⁵, C. Dallapiccola¹⁰², M. Dam⁴², G. D'amen²⁹, V. D'Amico^{76a,76b}, J. Damp⁹⁹, J. R. Dandoy¹²⁷, M. F. Daneri³⁰, M. Danninger¹⁴¹, V. Dao³⁶, G. Darbo^{57b}, S. Darmora⁶, S. J. Das^{29.af}, A. Dattagupta¹²², S. D'Auria^{70a,70b}, C. David^{155b}, T. Davidek¹³², D. R. Davis⁵¹, B. Davis-Purcell³⁴, I. Dawson⁹³, K. De⁸, R. De Asmundis^{71a}, M. De Beurs¹¹³, S. De Castro^{23a,23b}, N. De Groot¹¹², P. de Jong¹¹³, H. De la Torre¹⁰⁶, A. De Maria^{14c}, A. De Salvo^{74a}, U. De Sanctis^{75a,75b}, M. De Santis^{75a,75b}, A. De Santo¹⁴⁵, J. B. De Vivie De Regie⁶⁰, D. V. Dedovich³⁸, J. Degens¹¹³, A. M. Deiana⁴⁴, F. Del Corso^{23a,23b}, J. Del Peso⁹⁸, F. Del Rio^{63a}, F. Deliot¹³⁴, C. M. Delitzsch⁴⁹, M. Della Pietra^{71a,71b}, D. Della Volpe⁵⁶, A. Dell'Acqua³⁶, L. Dell'Asta^{70a,70b}, M. Delmastro⁴, P. A. Delsart⁶⁰, S. Demers¹⁷⁰, M. Demichev³⁸, S. P. Denisov³⁷, L. D'Eramo¹¹⁴, D. Derendarz⁸⁵, F. Derue¹²⁶, P. Dervan⁹¹, K. Desch²⁴, K. Dette¹⁵⁴, C. Deutsch²⁴, P. O. Deviveiros³⁶, F. A. Di Bello^{74a,74b}, A. Di Ciaccio^{75a,75b}, L. Di Ciaccio⁴, A. Di Domenico^{74a,74b}, C. Di Donato^{71a,71b}, A. Di Girolamo³⁶, G. Di Gregorio^{73a,73b}, A. Di Luca^{77a,77b}, B. Di Micco^{76a,76b}, R. Di Nardo^{76a,76b}, C. Diaconu¹⁰¹, F. A. Dias¹¹³, T. Dias Do Vale¹⁴¹, M. A. Diaz^{136a,136b}, F. G. Diaz Capriles²⁴, M. Didenko¹⁶¹, E. B. Diehl¹⁰⁵, L. Diehl⁵⁴, S. Díez Cornell⁴⁸, C. Diez Pardos¹⁴⁰, C. Dimitriadi^{24,159}, A. Dimitrievska^{17a}, W. Ding^{14b}, J. Dingfelder²⁴, I.-M. Dinu^{27b}, S. J. Dittmeier^{63b}, F. Dittus³⁶, F. Djama¹⁰¹, T. Djobava^{148b}, J. I. Djuvsland¹⁶, D. Dodsworth²⁶, C. Doglioni^{97,100}, J. Dolejsi¹³², Z. Dolezal¹³², M. Donadelli^{81c}, B. Dong^{62c}, J. Donini⁴⁰, A. D'Onofrio^{14c}, M. D'Onofrio⁹¹, J. Dopke¹³³, A. Doria^{71a}, M. T. Dova⁸⁹, A. T. Doyle⁵⁹, M. A. Draguet¹²⁵, E. Drechsler¹⁴¹, E. Dreyer¹⁶⁷, I. Drivas-koulouris¹⁰, A. S. Drobac¹⁵⁷, D. Du^{62a}, T. A. du Pree¹¹³, F. Dubinin³⁷, M. Dubovsky^{28a}, E. Duchovni¹⁶⁷, G. Duckeck¹⁰⁸, O. A. Ducu³⁶, D. Duda¹⁰⁹, A. Dudarev³⁶, M. D'uffizi¹⁰⁰, L. Duflot⁶⁶, M. Dührssen³⁶, C. Dülsen¹⁶⁹, A. E. Dumitriu^{27b}, M. Dunford^{63a}, S. Dungs⁴⁹, K. Dunne^{47a,47b}, A. Duperrin¹⁰¹, H. Duran Yildiz^{3a}, M. Düren⁵⁸, A. Durglishvili^{148b}, B. L. Dwyer¹¹⁴, G. I. Dyckes^{17a}, M. Dyndal^{84a}, S. Dysch¹⁰⁰, B. S. Dziedzic⁸⁵, B. Eckerova^{28a}, M. G. Eggleston⁵¹, E. Egidio Purcino De Souza^{81b}, L. F. Ehrke⁵⁶, G. Eigen¹⁶, K. Einsweiler^{17a}, T. Ekelof¹⁵⁹, P. A. Ekman⁹⁷, Y. El Ghazali^{35b}, H. El Jarrari^{35e,147}, A. El Moussaouy^{35a}, V. Ellajosyula¹⁵⁹, M. Ellert¹⁵⁹, F. Ellinghaus¹⁶⁹, A. A. Elliot⁹³, N. Ellis³⁶, J. Elmsheuser²⁹, M. Elsing³⁶, D. Emelianov¹³³, A. Emerman⁴¹, Y. Enari¹⁵², I. Ene^{17a}, S. Epari¹³, J. Erdmann⁴⁹, A. Ereditato¹⁹, P. A. Erland⁸⁵, M. Errenst¹⁶⁹, M. Escalier⁶⁶, C. Escobar¹⁶¹, E. Etzion¹⁵⁰, G. Evans^{129a}, H. Evans⁶⁷, M. O. Evans¹⁴⁵, A. Ezhilov³⁷, S. Ezzarqtouni^{35a}, F. Fabbri⁵⁹, L. Fabbri^{23a,23b}, G. Facini⁹⁵, V. Fadeyev¹³⁵, R. M. Fakhruddinov³⁷, S. Falciano^{74a}, P. J. Falke²⁴, S. Falke³⁶, J. Faltova¹³², Y. Fan^{14a}, Y. Fang^{14a,14d}, G. Fanourakis⁴⁶, M. Fanti^{70a,70b}, M. Faraj^{68a,68b}, A. Farbin⁸, A. Farilla^{76a}, T. Farooque¹⁰⁶, S. M. Farrington⁵², F. Fassi^{35e}, D. Fassouliotis⁹, M. Fauci Giannelli^{75a,75b}, W. J. Fawcett³², L. Fayard⁶⁶, O. L. Fedin^{37a}, G. Fedotov³⁷, M. Feickert¹⁶⁰

L. Feligioni¹⁰¹, A. Fell¹³⁸, D. E. Fellers¹²², C. Feng^{62b}, M. Feng^{14b}, M. J. Fenton¹⁵⁸, A. B. Fenyuk³⁷, L. Ferencz⁴⁸, S. W. Ferguson⁴⁵, J. Ferrando⁴⁸, A. Ferrari¹⁵⁹, P. Ferrari¹¹³, R. Ferrari^{72a}, D. Ferrere⁵⁶, C. Ferretti¹⁰⁵, F. Fiedler⁹⁹, A. Filipčić⁹², E. K. Filmer¹, F. Filthaut¹¹², M. C. N. Fiolhais^{129a,129c,b}, L. Fiorini¹⁶¹, F. Fischer¹⁴⁰, W. C. Fisher¹⁰⁶, T. Fitschen^{20,66}, I. Fleck¹⁴⁰, P. Fleischmann¹⁰⁵, T. Flick¹⁶⁹, L. Flores¹²⁷, M. Flores^{33d}, L. R. Flores Castillo^{64a}, F. M. Follega^{77a,77b}, N. Fomin¹⁶, J. H. Foo¹⁵⁴, B. C. Forland⁶⁷, A. Formica¹³⁴, A. C. Forti¹⁰⁰, E. Fortin¹⁰¹, A. W. Fortman⁶¹, M. G. Foti^{17a}, L. Fountas^{9,i}, D. Fournier⁶⁶, H. Fox⁹⁰, P. Francavilla^{73a,73b}, S. Francescato⁶¹, M. Franchini^{23a,23b}, S. Franchino^{63a}, D. Francis³⁶, L. Franco¹¹², L. Franconi¹⁹, M. Franklin⁶¹, G. Frattari²⁶, A. C. Freegard⁹³, P. M. Freeman²⁰, W. S. Freund^{81b}, N. Fritzsche⁵⁰, A. Froch⁵⁴, D. Froidevaux³⁶, J. A. Frost¹²⁵, Y. Fu^{62a}, M. Fujimoto¹¹⁷, E. Fullana Torregrosa^{161,*}, J. Fuster¹⁶¹, A. Gabrielli^{23a,23b}, A. Gabrielli³⁶, P. Gadow⁴⁸, G. Gagliardi^{57a,57b}, L. G. Gagnon^{17a}, G. E. Gallardo¹²⁵, E. J. Gallas¹²⁵, B. J. Gallop¹³³, R. Gamboa Goni⁹³, K. K. Gan¹¹⁸, S. Ganguly¹⁵², J. Gao^{62a}, Y. Gao⁵², F. M. Garay Walls^{136a,136b}, B. Garcia^{29,af}, C. García¹⁶¹, J. E. García Navarro¹⁶¹, J. A. García Pascual^{14a}, M. Garcia-Sciveres^{17a}, R. W. Gardner³⁹, D. Garg⁷⁹, R. B. Garg^{142,ai}, S. Gargiulo⁵⁴, C. A. Garner¹⁵⁴, V. Garonne²⁹, S. J. Gasiorowski¹³⁷, P. Gaspar^{81b}, G. Gaudio^{72a}, P. Gauzzi^{74a,74b}, I. L. Gavrilenko³⁷, A. Gavriluk³⁷, C. Gay¹⁶², G. Gaycken⁴⁸, E. N. Gazis¹⁰, A. A. Geanta^{27b}, C. M. Gee¹³⁵, J. Geisen⁹⁷, M. Geisen⁹⁹, C. Gemme^{57b}, M. H. Genest⁶⁰, S. Gentile^{74a,74b}, S. George⁹⁴, W. F. George²⁰, T. Gerialis⁴⁶, L. O. Gerlach⁵⁵, P. Gessinger-Befurt³⁶, M. Ghasemi Bostanabad¹⁶³, M. Ghneimat¹⁴⁰, A. Ghosal¹⁴⁰, A. Ghosh¹⁵⁸, A. Ghosh⁷, B. Giacobbe^{23b}, S. Giagu^{74a,74b}, N. Giangiacomi¹⁵⁴, P. Giannetti^{73a}, A. Giannini^{62a}, S. M. Gibson⁹⁴, M. Gignac¹³⁵, D. T. Gil^{84b}, A. K. Gilbert^{84a}, B. J. Gilbert⁴¹, D. Gillberg³⁴, G. Gilles¹¹³, N. E. K. Gillwald⁴⁸, L. Ginabat¹²⁶, D. M. Gingrich^{2,ac}, M. P. Giordani^{68a,68c}, P. F. Giraud¹³⁴, G. Giugliarelli^{68a,68c}, D. Giugni^{70a}, F. Giuli³⁶, I. Gkialas^{9,i}, L. K. Gladilin³⁷, C. Glasman⁹⁸, G. R. Gledhill¹²², M. Glisic¹²², I. Gnesi^{43b,e}, Y. Go^{29,af}, M. Goblirsch-Kolb²⁶, D. Godin¹⁰⁷, S. Goldfarb¹⁰⁴, T. Golling⁵⁶, M. G. D. Gololo^{33g}, D. Golubkov³⁷, J. P. Gombas¹⁰⁶, A. Gomes^{129a,129b}, A. J. Gomez Delegido¹⁶¹, R. Goncalves Gama⁵⁵, R. Gonçalves^{129a,129c}, G. Gonella¹²², L. Gonella²⁰, A. Gongadze³⁸, F. Gonnella²⁰, J. L. Gonski⁴¹, S. González de la Hoz¹⁶¹, S. Gonzalez Fernandez¹³, R. Gonzalez Lopez⁹¹, C. Gonzalez Renteria^{17a}, R. Gonzalez Suarez¹⁵⁹, S. Gonzalez-Sevilla⁵⁶, G. R. Gonzalvo Rodriguez¹⁶¹, R. Y. González Andana⁵², L. Goossens³⁶, N. A. Gorasia²⁰, P. A. Gorbounov³⁷, B. Gorini³⁶, E. Gorini^{69a,69b}, A. Gorišek⁹², A. T. Goshaw⁵¹, M. I. Gostkin³⁸, C. A. Gottardo¹¹², M. Goughri^{35b}, V. Goumarre⁴⁸, A. G. Goussiou¹³⁷, N. Govender^{33c}, C. Goy⁴, I. Grabowska-Bold^{84a}, K. Graham³⁴, E. Gramstad¹²⁴, S. Grancagnolo¹⁸, M. Grandi¹⁴⁵, V. Gratchev^{37,*}, P. M. Gravila^{27f}, F. G. Gravili^{69a,69b}, H. M. Gray^{17a}, M. Greco^{69a,69b}, C. Grefe²⁴, I. M. Gregor⁴⁸, P. Grenier¹⁴², C. Grieco¹³, A. A. Grillo¹³⁵, K. Grimm^{31,m}, S. Grinstein^{13,t}, J.-F. Grivaz⁶⁶, E. Gross¹⁶⁷, J. Grosse-Knetter⁵⁵, C. Grud¹⁰⁵, A. Grummer¹¹¹, J. C. Grundy¹²⁵, L. Guan¹⁰⁵, W. Guan¹⁶⁸, C. Gubbels¹⁶², J. G. R. Guerrero Rojas¹⁶¹, G. Guerrieri^{68a,68c}, F. Guescini¹⁰⁹, R. Gugel⁹⁹, J. A. M. Guhit¹⁰⁵, A. Guida⁴⁸, T. Guillemain⁴, E. Guilloton^{133,165}, S. Guindon³⁶, F. Guo^{14a,14d}, J. Guo^{62c}, L. Guo⁶⁶, Y. Guo¹⁰⁵, R. Gupta⁴⁸, S. Gurbuz²⁴, G. Gustavo³⁶, M. Guth⁵⁶, P. Gutierrez¹¹⁹, L. F. Gutierrez Zagazeta¹²⁷, C. Gutschow⁹⁵, C. Guyot¹³⁴, C. Gwenlan¹²⁵, C. B. Gwilliam⁹¹, E. S. Haaland¹²⁴, A. Haas¹¹⁶, M. Habedank⁴⁸, C. Haber^{17a}, H. K. Hadavand⁸, A. Hadeef⁹⁹, S. Hadzic¹⁰⁹, M. Haleem¹⁶⁴, J. Haley¹²⁰, J. J. Hall¹³⁸, G. D. Hallowell¹⁰¹, L. Halser¹⁹, K. Hamano¹⁶³, H. Hamdaoui^{35e}, M. Hamer²⁴, G. N. Hamity⁵², J. Han^{62b}, K. Han^{62a}, L. Han^{14c}, L. Han^{62a}, S. Han^{17a}, Y. F. Han¹⁵⁴, K. Hanagaki⁸², M. Hance¹³⁵, D. A. Hangal^{41,y}, M. D. Hank³⁹, R. Hankache¹⁰⁰, J. B. Hansen⁴², J. D. Hansen⁴², P. H. Hansen⁴², K. Hara¹⁵⁶, D. Harada⁵⁶, T. Harenberg¹⁶⁹, S. Harkusha³⁷, Y. T. Harris¹²⁵, P. F. Harrison¹⁶⁵, N. M. Hartman¹⁴², N. M. Hartmann¹⁰⁸, Y. Hasegawa¹³⁹, A. Hasib⁵², S. Haug¹⁹, R. Hauser¹⁰⁶, M. Havranek¹³¹, C. M. Hawkes²⁰, R. J. Hawkins³⁶, S. Hayashida¹¹⁰, D. Hayden¹⁰⁶, C. Hayes¹⁰⁵, R. L. Hayes¹⁶², C. P. Hays¹²⁵, J. M. Hays⁹³, H. S. Hayward⁹¹, F. He^{62a}, Y. He¹⁵³, Y. He¹²⁶, M. P. Heath⁵², V. Hedberg⁹⁷, A. L. Heggelund¹²⁴, N. D. Hehir⁹³, C. Heidegger⁵⁴, K. K. Heidegger⁵⁴, W. D. Heidorn⁸⁰, J. Heilman³⁴, S. Heim⁴⁸, T. Heim^{17a}, J. G. Heinlein¹²⁷, J. J. Heinrich¹²², L. Heinrich³⁶, J. Hejbal¹³⁰, L. Helary⁴⁸, A. Held¹¹⁶, S. Hellesund¹²⁴, C. M. Helling¹⁶², S. Hellman^{47a,47b}, C. Helsen³⁶, R. C. W. Henderson⁹⁰, L. Henkelmann³², A. M. Henriques Correia³⁶, H. Herde¹⁴², Y. Hernández Jiménez¹⁴⁴, H. Herr⁹⁹, M. G. Herrmann¹⁰⁸, T. Herrmann⁵⁰, G. Herten⁵⁴, R. Hertenberger¹⁰⁸, L. Hervas³⁶, N. P. Hessey^{155a}, H. Hibi⁸³, E. Higón-Rodríguez¹⁶¹, S. J. Hillier²⁰, I. Hinchliffe^{17a}, F. Hinterkeuser²⁴, M. Hirose¹²³, S. Hirose¹⁵⁶, D. Hirschbuehl¹⁶⁹, T. G. Hitchings¹⁰⁰, B. Hiti⁹², J. Hobbs¹⁴⁴, R. Hobincu^{27e}, N. Hod¹⁶⁷, M. C. Hodgkinson¹³⁸, B. H. Hodgkinson³², A. Hoecker³⁶, J. Hofel⁴⁸, D. Hohn⁵⁴, T. Holm²⁴

M. Holzbock¹⁰⁹, L. B. A. H. Hommels³², B. P. Honan¹⁰⁰, J. Hong^{62c}, T. M. Hong¹²⁸, Y. Hong⁵⁵, J. C. Honig⁵⁴, A. Hönle¹⁰⁹, B. H. Hooberman¹⁶⁰, W. H. Hopkins⁶, Y. Horii¹¹⁰, S. Hou¹⁴⁷, J. Howarth⁵⁹, J. Hoya⁸⁹, M. Hrabovsky¹²¹, A. Hrynevich³⁷, T. Hryn'ova⁴, P. J. Hsu⁶⁵, S.-C. Hsu¹³⁷, Q. Hu^{41,y}, Y. F. Hu^{14a,14d,ae}, D. P. Huang⁹⁵, S. Huang^{64b}, X. Huang^{14c}, Y. Huang^{62a}, Y. Huang^{14a}, Z. Huang¹⁰⁰, Z. Hubacek¹³¹, M. Huebner²⁴, F. Huegging²⁴, T. B. Huffman¹²⁵, M. Huhtinen³⁶, S. K. Huiberts¹⁶, R. Hulsken¹⁰³, N. Huseynov^{12,a}, J. Huston¹⁰⁶, J. Huth⁶¹, R. Hyneman¹⁴², S. Hyrych^{28a}, G. Iacobucci⁵⁶, G. Iakovidis²⁹, I. Ibragimov¹⁴⁰, L. Iconomidou-Fayard⁶⁶, P. Iengo^{71a,71b}, R. Iguchi¹⁵², T. Iizawa⁵⁶, Y. Ikegami⁸², A. Ilg¹⁹, N. Ilic¹⁵⁴, H. Imam^{35a}, T. Ingebretsen Carlson^{47a,47b}, G. Introzzi^{72a,72b}, M. Iodice^{76a}, V. Ippolito^{74a,74b}, M. Ishino¹⁵², W. Islam¹⁶⁸, C. Issever^{18,48}, S. Istin^{21a,ag}, H. Ito¹⁶⁶, J. M. Iturbe Ponce^{64a}, R. Iuppa^{77a,77b}, A. Ivina¹⁶⁷, J. M. Izen⁴⁵, V. Izzo^{71a}, P. Jacka^{130,131}, P. Jackson¹, R. M. Jacobs⁴⁸, B. P. Jaeger¹⁴¹, C. S. Jagfeld¹⁰⁸, G. Jäkel¹⁶⁹, K. Jakobs⁵⁴, T. Jakoubek¹⁶⁷, J. Jamieson⁵⁹, K. W. Janas^{84a}, G. Jarlskog⁹⁷, A. E. Jaspán⁹¹, T. Javůrek³⁶, M. Javurkova¹⁰², F. Jeanneau¹³⁴, L. Jeanty¹²², J. Jejelava^{148a,x}, P. Jenni^{54,f}, C. E. Jessiman³⁴, S. Jézéquel⁴, J. Jia¹⁴⁴, X. Jia⁶¹, X. Jia^{14a,14d}, Z. Jia^{14c}, Y. Jiang^{62a}, S. Jiggins⁵², J. Jimenez Pena¹⁰⁹, S. Jin^{14c}, A. Jinaru^{27b}, O. Jinnouchi¹⁵³, H. Jivan^{33g}, P. Johansson¹³⁸, K. A. Johns⁷, C. A. Johnson⁶⁷, D. M. Jones³², E. Jones¹⁶⁵, R. W. L. Jones⁹⁰, T. J. Jones⁹¹, J. Jovicevic¹⁵, X. Ju^{17a}, J. J. Junggeburth³⁶, A. Juste Rozas^{13,t}, S. Kabana^{136e}, A. Kaczmarek⁸⁵, M. Kado^{74a,74b}, H. Kagan¹¹⁸, M. Kagan¹⁴², A. Kahn⁴¹, A. Kahn¹²⁷, C. Kahra⁹⁹, T. Kaji¹⁶⁶, E. Kajomovitz¹⁴⁹, N. Kakati¹⁶⁷, C. W. Kalderon²⁹, A. Kamenshchikov¹⁵⁴, N. J. Kang¹³⁵, Y. Kano¹¹⁰, D. Kar^{33g}, K. Karava¹²⁵, M. J. Kareem^{155b}, E. Karentzos⁵⁴, I. Karkanas¹⁵¹, S. N. Karpov³⁸, Z. M. Karpova³⁸, V. Kartvelishvili⁹⁰, A. N. Karyukhin³⁷, E. Kasimi¹⁵¹, C. Kato^{62d}, J. Katzy⁴⁸, S. Kaur³⁴, K. Kawade¹³⁹, K. Kawagoe⁸⁸, T. Kawaguchi¹¹⁰, T. Kawamoto¹³⁴, G. Kawamura⁵⁵, E. F. Kay¹⁶³, F. I. Kaya¹⁵⁷, S. Kazakos¹³, V. F. Kazanin³⁷, Y. Ke¹⁴⁴, J. M. Keaveney^{33a}, R. Keeler¹⁶³, G. V. Kehris⁶¹, J. S. Keller³⁴, A. S. Kelly⁹⁵, D. Kelsey¹⁴⁵, J. J. Kempster²⁰, J. Kendrick²⁰, K. E. Kennedy⁴¹, O. Kepka¹³⁰, B. P. Kerridge¹⁶⁵, S. Kersten¹⁶⁹, B. P. Kerševan⁹², L. Keszeghova^{28a}, S. Kitabchi Haghghat¹⁵⁴, M. Khandoga¹²⁶, A. Khanov¹²⁰, A. G. Kharlamov³⁷, T. Kharlamova³⁷, E. E. Khoda¹³⁷, T. J. Khoo¹⁸, G. Khorauli¹⁶⁴, J. Khubua^{148b}, Y. A. R. Khwairar⁶⁶, M. Kiehn³⁶, A. Kilgallon¹²², D. W. Kim^{47a,47b}, E. Kim¹⁵³, Y. K. Kim³⁹, N. Kimura⁹⁵, A. Kirchhoff⁵⁵, D. Kirchmeier⁵⁰, C. Kirfel²⁴, J. Kirk¹³³, A. E. Kiryunin¹⁰⁹, T. Kishimoto¹⁵², D. P. Kisiuk¹⁵⁴, C. Kitsaki¹⁰, O. Kivernyk²⁴, M. Klassen^{63a}, C. Klein³⁴, L. Klein¹⁶⁴, M. H. Klein¹⁰⁵, M. Klein⁹¹, U. Klein⁹¹, P. Klimek³⁶, A. Klimentov²⁹, F. Klimpel¹⁰⁹, T. Klingl²⁴, T. Klioutchnikova³⁶, F. F. Klitzner¹⁰⁸, P. Kluit¹¹³, S. Kluth¹⁰⁹, E. Kneringer⁷⁸, T. M. Knight¹⁵⁴, A. Knue⁵⁴, D. Kobayashi⁸⁸, R. Kobayashi⁸⁶, M. Kocian¹⁴², T. Kodama¹⁵², P. Kodyš¹³², D. M. Koeck¹⁴⁵, P. T. Koenig²⁴, T. Koffas³⁴, N. M. Köhler³⁶, M. Kolb¹³⁴, I. Koletsou⁴, T. Komarek¹²¹, K. Köneke⁵⁴, A. X. Y. Kong¹, T. Kono¹¹⁷, N. Konstantinidis⁹⁵, B. Konya⁹⁷, R. Kopeliansky⁶⁷, S. Koperny^{84a}, K. Korcyl⁸⁵, K. Kordas¹⁵¹, G. Koren¹⁵⁰, A. Korn⁹⁵, S. Korn⁵⁵, I. Korolkov¹³, N. Korotkova³⁷, B. Kortman¹¹³, O. Kortner¹⁰⁹, S. Kortner¹⁰⁹, W. H. Kostecka¹¹⁴, V. V. Kostyukhin¹⁴⁰, A. Kotsokechagia⁶⁶, A. Kotwal⁵¹, A. Koulouris³⁶, A. Kourkoumeli-Charalampidi^{72a,72b}, C. Kourkoumelis⁹, E. Kourlitis⁶, O. Kovanda¹⁴⁵, R. Kowalewski¹⁶³, W. Kozanecki¹³⁴, A. S. Kozhin³⁷, V. A. Kramarenko³⁷, G. Kramberger⁹², P. Kramer⁹⁹, M. W. Krasny¹²⁶, A. Krasznahorkay³⁶, J. A. Kremer⁹⁹, J. Kretzschmar⁹¹, K. Kreul¹⁸, P. Krieger¹⁵⁴, F. Krieter¹⁰⁸, S. Krishnamurthy¹⁰², A. Krishnan^{63b}, M. Krivos¹³², K. Krizka^{17a}, K. Kroeninger⁴⁹, H. Kroha¹⁰⁹, J. Kroll¹³⁰, J. Kroll¹²⁷, K. S. Krowpman¹⁰⁶, U. Kruchonak³⁸, H. Krüger²⁴, N. Krumnack⁸⁰, M. C. Kruse⁵¹, J. A. Krzysiak⁸⁵, A. Kubota¹⁵³, O. Kuchinskaia³⁷, S. Kuday^{3a}, D. Kuechler⁴⁸, J. T. Kuechler⁴⁸, S. Kuehn³⁶, T. Kuhl⁴⁸, V. Kukhtin³⁸, Y. Kulchitsky^{37,a}, S. Kuleshov^{136b,136d}, M. Kumar^{33g}, N. Kumari¹⁰¹, M. Kuna⁶⁰, A. Kupco¹³⁰, T. Kupfer⁴⁹, A. Kupich³⁷, O. Kuprash⁵⁴, H. Kurashige⁸³, L. L. Kurchaninov^{155a}, Y. A. Kurochkin³⁷, A. Kurova³⁷, E. S. Kuwertz³⁶, M. Kuze¹⁵³, A. K. Kvam¹⁰², J. Kvita¹²¹, T. Kwan¹⁰³, K. W. Kwok^{64a}, C. Lacasta¹⁶¹, F. Lacava^{74a,74b}, H. Lacker¹⁸, D. Lacour¹²⁶, N. N. Lad⁹⁵, E. Ladygin³⁸, B. Laforge¹²⁶, T. Lagouri^{136e}, S. Lai⁵⁵, I. K. Lakomic^{84a}, N. Lalloue⁶⁰, J. E. Lambert¹¹⁹, S. Lammers⁶⁷, W. Lampf⁷, C. Lampoudis¹⁵¹, A. N. Lancaster¹¹⁴, E. Lançon²⁹, U. Landgraf⁵⁴, M. P. J. Landon⁹³, V. S. Lang⁵⁴, R. J. Langenberg¹⁰², A. J. Lankford¹⁵⁸, F. Lanni²⁹, K. Lantzsch²⁴, A. Lanza^{72a}, A. Lapertosa^{57a,57b}, J. F. Laporte¹³⁴, T. Lari^{70a}, F. Lasagni Manghi^{23b}, M. Lassnig³⁶, V. Latonova¹³⁰, T. S. Lau^{64a}, A. Laudrain⁹⁹, A. Laurier³⁴, S. D. Lawlor⁹⁴, Z. Lawrence¹⁰⁰, M. Lazzaroni^{70a,70b}, B. Le¹⁰⁰, B. Leban⁹², A. Lebedev⁸⁰, M. LeBlanc³⁶, T. LeCompte⁶, F. Ledroit-Guillon⁶⁰, A. C. A. Lee⁹⁵, G. R. Lee¹⁶, L. Lee⁶¹, S. C. Lee¹⁴⁷, S. Lee^{47a,47b}, L. L. Leeuw^{33c}, H. P. Lefebvre⁹⁴, M. Lefebvre¹⁶³, C. Leggett^{17a}, K. Lehmann¹⁴¹, G. Lehmann Miotto³⁶, W. A. Leight¹⁰², A. Leisos^{151,s}, M. A. L. Leite^{81c}

H. Nanjo¹²³, R. Narayan⁴⁴, E. A. Narayanan¹¹¹, I. Naryshkin³⁷, M. Naseri³⁴, C. Nass²⁴, G. Navarro^{22a}, J. Navarro-Gonzalez¹⁶¹, R. Nayak¹⁵⁰, P. Y. Nechaeva³⁷, F. Nechansky⁴⁸, T. J. Neep²⁰, A. Negri^{72a,72b}, M. Negrini^{23b}, C. Nellist¹¹², C. Nelson¹⁰³, K. Nelson¹⁰⁵, S. Nemecek¹³⁰, M. Nessi^{36g}, M. S. Neubauer¹⁶⁰, F. Neuhaus⁹⁹, J. Neundorff⁴⁸, R. Newhouse¹⁶², P. R. Newman²⁰, C. W. Ng¹²⁸, Y. S. Ng¹⁸, Y. W. Y. Ng¹⁵⁸, B. Ngair^{35e}, H. D. N. Nguyen¹⁰⁷, R. B. Nickerson¹²⁵, R. Nicolaidou¹³⁴, J. Nielsen¹³⁵, M. Niemeyer⁵⁵, N. Nikiforou³⁶, V. Nikolaenko^{37a}, I. Nikolic-Audit¹²⁶, K. Nikolopoulos²⁰, P. Nilsson²⁹, H. R. Nindhito⁵⁶, A. Nisati^{74a}, N. Nishu², R. Nisius¹⁰⁹, J.-E. Nitschke⁵⁰, E. K. Nkadimeng^{33g}, S. J. Noacco Rosende⁸⁹, T. Nobe¹⁵², D. L. Noel³², Y. Noguchi⁸⁶, T. Nommensen¹⁴⁶, M. A. Nomura²⁹, M. B. Norfolk¹³⁸, R. R. B. Norisam⁹⁵, B. J. Norman³⁴, J. Novak⁹², T. Novak⁴⁸, O. Novgorodova⁵⁰, L. Novotny¹³¹, R. Novotny¹¹¹, L. Nozka¹²¹, K. Ntekas¹⁵⁸, E. Nurse⁹⁵, F. G. Oakham^{34,ac}, J. Ocariz¹²⁶, A. Ochi⁸³, I. Ochoa^{129a}, S. Oda⁸⁸, S. Oerdek¹⁵⁹, A. Ogrodnik^{84a}, A. Oh¹⁰⁰, C. C. Ohm¹⁴³, H. Oide¹⁵³, R. Oishi¹⁵², M. L. Ojeda⁴⁸, Y. Okazaki⁸⁶, M. W. O'Keefe⁹¹, Y. Okumura¹⁵², A. Olariu^{27b}, L. F. Oleiro Seabra^{129a}, S. A. Olivares Pino^{136e}, D. Oliveira Damazio²⁹, D. Oliveira Goncalves^{81a}, J. L. Oliver¹⁵⁸, M. J. R. Olsson¹⁵⁸, A. Olszewski⁸⁵, J. Olszowska^{85,*}, Ö. O. Öncel⁵⁴, D. C. O'Neil¹⁴¹, A. P. O'Neill¹⁹, A. Onofre^{129a,129e}, P. U. E. Onyisi¹¹, M. J. Oreglia³⁹, G. E. Orellana⁸⁹, D. Orestano^{76a,76b}, N. Orlando¹³, R. S. Orr¹⁵⁴, V. O'Shea⁵⁹, R. Ospanov^{62a}, G. Otero y Garzon³⁰, H. Otono⁸⁸, P. S. Ott^{63a}, G. J. Ottino^{17a}, M. Ouchrif^{35d}, J. Ouellette^{29,af}, F. Ould-Saada¹²⁴, M. Owen⁵⁹, R. E. Owen¹³³, K. Y. Oyulmaz^{21a}, V. E. Ozcan^{21a}, N. Ozturk⁸, S. Ozturk^{21d}, J. Pacalt¹²¹, H. A. Pacey³², K. Pachal⁵¹, A. Pacheco Pages¹³, C. Padilla Aranda¹³, G. Padovano^{74a,74b}, S. Pagan Griso^{17a}, G. Palacino⁶⁷, A. Palazzo^{69a,69b}, S. Palazzo⁵², S. Palestini³⁶, M. Palka^{84b}, J. Pan¹⁷⁰, D. K. Panchal¹¹, C. E. Pandini¹¹³, J. G. Panduro Vazquez⁹⁴, P. Pani⁴⁸, G. Panizzo^{68a,68c}, L. Paolozzi⁵⁶, C. Papadatos¹⁰⁷, S. Parajuli⁴⁴, A. Paramonov⁶, C. Paraskevopoulos¹⁰, D. Paredes Hernandez^{64b}, T. H. Park¹⁵⁴, M. A. Parker³², F. Parodi^{57a,57b}, E. W. Parrish¹¹⁴, V. A. Parrish⁵², J. A. Parsons⁴¹, U. Parzefall⁵⁴, B. Pascual Dias¹⁰⁷, L. Pascual Dominguez¹⁵⁰, V. R. Pascuzzi^{17a}, F. Pasquali¹¹³, E. Pasqualucci^{74a}, S. Passaggio^{57b}, F. Pastore⁹⁴, P. Pasuwan^{47a,47b}, J. R. Pater¹⁰⁰, J. Patton⁹¹, T. Pauly³⁶, J. Parkes¹⁴², M. Pedersen¹²⁴, R. Pedro^{129a}, S. V. Peleganchuk³⁷, O. Penc¹³⁰, C. Peng^{64b}, H. Peng^{62a}, M. Penzin³⁷, B. S. Peralva^{81a}, A. P. Pereira Peixoto⁶⁰, L. Pereira Sanchez^{47a,47b}, D. V. Perepelitsa^{29,af}, E. Perez Codina^{155a}, M. Perganti¹⁰, L. Perini^{70a,70b,*}, H. Pernegger³⁶, S. Perrella³⁶, A. Perrevoort¹¹², O. Perrin⁴⁰, K. Peters⁴⁸, R. F. Y. Peters¹⁰⁰, B. A. Petersen³⁶, T. C. Petersen⁴², E. Petit¹⁰¹, V. Petousis¹³¹, C. Petridou¹⁵¹, A. Petrukhin¹⁴⁰, M. Pettee^{17a}, N. E. Pettersson³⁶, A. Petukhov³⁷, K. Petukhova¹³², A. Peyaud¹³⁴, R. Pezoa^{136f}, L. Pezzotti³⁶, G. Pezzullo¹⁷⁰, T. Pham¹⁰⁴, P. W. Phillips¹³³, M. W. Phipps¹⁶⁰, G. Piacquadio¹⁴⁴, E. Pianori^{17a}, F. Piazza^{70a,70b}, R. Piegai³⁰, D. Pietreanu^{27b}, A. D. Pilkington¹⁰⁰, M. Pinamonti^{68a,68c}, J. L. Pinfold², B. C. Pinheiro Pereira^{129a}, C. Pitman Donaldson⁹⁵, D. A. Pizzi³⁴, L. Pizzimento^{75a,75b}, A. Pizzini¹¹³, M.-A. Pleier²⁹, V. Plesanovs⁵⁴, V. Pleskot¹³², E. Plotnikova³⁸, G. Poddar⁴, R. Poettgen⁹⁷, R. Poggi⁵⁶, L. Poggioli¹²⁶, I. Pogrebnyak¹⁰⁶, D. Pohl²⁴, I. Pokharel⁵⁵, S. Polacek¹³², G. Polesello^{72a}, A. Poley^{141,155a}, R. Polifka¹³¹, A. Polini^{23b}, C. S. Pollard¹²⁵, Z. B. Pollock¹¹⁸, V. Polychronakos²⁹, D. Ponomarenko³⁷, L. Pontecorvo³⁶, S. Popa^{27a}, G. A. Popeneciu^{27d}, D. M. Portillo Quintero^{155a}, S. Pospisil¹³¹, P. Postolache^{27c}, K. Potamianos¹²⁵, I. N. Potrap³⁸, C. J. Potter³², H. Potti¹, T. Poulsen⁴⁸, J. Poveda¹⁶¹, G. Pownall⁴⁸, M. E. Pozo Astigarraga³⁶, A. Prades Ibanez¹⁶¹, M. M. Prapa⁴⁶, J. Pretel⁵⁴, D. Price¹⁰⁰, M. Primavera^{69a}, M. A. Principe Martin⁹⁸, M. L. Proffitt¹³⁷, N. Proklova³⁷, K. Prokofiev^{64c}, G. Proto^{75a,75b}, S. Protopopescu²⁹, J. Proudfoot⁶, M. Przybycien^{84a}, J. E. Puddefoot¹³⁸, D. Pudza³⁷, P. Puzo⁶⁶, D. Pyatiizbyantseva³⁷, J. Qian¹⁰⁵, Y. Qin¹⁰⁰, T. Qiu⁹³, A. Quadt⁵⁵, M. Queitsch-Maitland²⁴, G. Rabanal Bolanos⁶¹, D. Rafanoharana⁵⁴, F. Ragusa^{70a,70b}, J. L. Rainbolt³⁹, J. A. Raine⁵⁶, S. Rajagopalan²⁹, E. Ramakoti³⁷, K. Ran^{14a,14d}, V. Raskina¹²⁶, D. F. Rassloff^{63a}, S. Rave⁹⁹, B. Ravina⁵⁹, I. Ravinovich¹⁶⁷, M. Raymond³⁶, A. L. Read¹²⁴, N. P. Readoff¹³⁸, D. M. Rebuffi^{72a,72b}, G. Redlinger²⁹, K. Reeves⁴⁵, J. A. Reidelsturz¹⁶⁹, D. Reikher¹⁵⁰, A. Reiss⁹⁹, A. Rej¹⁴⁰, C. Rembser³⁶, A. Renardi⁴⁸, M. Renda^{27b}, M. B. Rendel¹⁰⁹, A. G. Rennie⁵⁹, S. Resconi^{70a}, M. Ressegotti^{57a,57b}, E. D. Resseguie^{17a}, S. Rettie⁹⁵, B. Reynolds¹¹⁸, E. Reynolds^{17a}, M. Rezaei Estabragh¹⁶⁹, O. L. Rezanova³⁷, P. Reznicek¹³², E. Ricci^{77a,77b}, R. Richter¹⁰⁹, S. Richter^{47a,47b}, E. Richter-Was^{84b}, M. Ridel¹²⁶, P. Rieck¹¹⁶, P. Riedler³⁶, M. Rijssenbeek¹⁴⁴, A. Rimoldi^{72a,72b}, M. Rimoldi⁴⁸, L. Rinaldi^{23a,23b}, T. T. Rinn²⁹, M. P. Rinnagel¹⁰⁸, G. Ripellino¹⁴³, I. Riu¹³, P. Rivadeneira⁴⁸, J. C. Rivera Vergara¹⁶³, F. Rizatdinova¹²⁰, E. Rizvi⁹³, C. Rizzi⁵⁶, B. A. Roberts¹⁶⁵, B. R. Roberts^{17a}, S. H. Robertson^{103,v}, M. Robin⁴⁸, D. Robinson³², C. M. Robles Gajardo^{136f}, M. Robles Manzano⁹⁹, A. Robson⁵⁹, A. Rocchi^{75a,75b}, C. Roda^{73a,73b}, S. Rodriguez Bosca^{63a}, Y. Rodriguez Garcia^{22a}, A. Rodriguez Rodriguez⁵⁴

A. M. Rodríguez Vera^{155b}, S. Roe³⁶, J. T. Roemer¹⁵⁸, A. R. Roepe-Gier¹¹⁹, J. Roggel¹⁶⁹, O. Røhne¹²⁴, R. A. Rojas¹⁶³, B. Roland⁵⁴, C. P. A. Roland⁶⁷, J. Roloff²⁹, A. Romaniouk³⁷, E. Romano^{72a,72b}, M. Romano^{23b}, A. C. Romero Hernandez¹⁶⁰, N. Rompotis⁹¹, L. Roos¹²⁶, S. Rosati^{74a}, B. J. Rosser³⁹, E. Rossi⁴, E. Rossi^{71a,71b}, L. P. Rossi^{57b}, L. Rossini⁴⁸, R. Rosten¹¹⁸, M. Rotaru^{27b}, B. Rottler⁵⁴, D. Rousseau⁶⁶, D. Rouso³², G. Rovelli^{72a,72b}, A. Roy¹⁶⁰, A. Rozanov¹⁰¹, Y. Rozen¹⁴⁹, X. Ruan^{33g}, A. Rubio Jimenez¹⁶¹, A. J. Ruby⁹¹, T. A. Ruggeri¹, F. Rühr⁵⁴, A. Ruiz-Martinez¹⁶¹, A. Rummeler³⁶, Z. Rurikova⁵⁴, N. A. Rusakovich³⁸, H. L. Russell¹⁶³, J. P. Rutherford⁷, S. Rutherford Colmenares³², E. M. Rüttinger¹³⁸, K. Rybacki⁹⁰, M. Rybar¹³², E. B. Rye¹²⁴, A. Ryzhov³⁷, J. A. Sabater Iglesias⁵⁶, P. Sabatini¹⁶¹, L. Sabetta^{74a,74b}, H. F.-W. Sadrozinski¹³⁵, F. Safai Tehrani^{74a}, B. Safarzadeh Samani¹⁴⁵, M. Safdari¹⁴², S. Saha¹⁰³, M. Sahinsky¹⁰⁹, M. Saimpert¹³⁴, M. Saito¹⁵², T. Saito¹⁵², D. Salamani³⁶, G. Salamanna^{76a,76b}, A. Salnikov¹⁴², J. Salt¹⁶¹, A. Salvador Salas¹³, D. Salvatore^{43a,43b}, F. Salvatore¹⁴⁵, A. Salzburger³⁶, D. Sammel⁵⁴, D. Sampsonidis¹⁵¹, D. Sampsonidou^{62c,62d}, J. Sánchez¹⁶¹, A. Sanchez Pineda⁴, V. Sanchez Sebastian¹⁶¹, H. Sandaker¹²⁴, C. O. Sander⁴⁸, J. A. Sandesara¹⁰², M. Sandhoff¹⁶⁹, C. Sandoval^{22b}, D. P. C. Sankey¹³³, A. Sansoni⁵³, L. Santi^{74a,74b}, C. Santoni⁴⁰, H. Santos^{129a,129b}, S. N. Santpur^{17a}, A. Santra¹⁶⁷, K. A. Saoucha¹³⁸, J. G. Saraiva^{129a,129d}, J. Sardain¹⁰¹, O. Sasaki⁸², K. Sato¹⁵⁶, C. Sauer^{63b}, F. Sauerburger⁵⁴, E. Sauvan⁴, P. Savard^{154.ac}, R. Sawada¹⁵², C. Sawyer¹³³, L. Sawyer⁹⁶, I. Sayago Galvan¹⁶¹, C. Sbarra^{23b}, A. Sbrizzi^{23a,23b}, T. Scanlon⁹⁵, J. Schaarschmidt¹³⁷, P. Schacht¹⁰⁹, D. Schaefer³⁹, U. Schäfer⁹⁹, A. C. Schaffer⁶⁶, D. Schaile¹⁰⁸, R. D. Schamberger¹⁴⁴, E. Schanet¹⁰⁸, C. Scharf¹⁸, V. A. Schegelsky³⁷, D. Scheirich¹³², F. Schenck¹⁸, M. Schernau¹⁵⁸, C. Scheulen⁵⁵, C. Schiavi^{57a,57b}, Z. M. Schillaci²⁶, E. J. Schioppa^{69a,69b}, M. Schioppa^{43a,43b}, B. Schlag⁹⁹, K. E. Schleicher⁵⁴, S. Schlenker³⁶, K. Schmieden⁹⁹, C. Schmitt⁹⁹, S. Schmitt⁴⁸, L. Schoeffel¹³⁴, A. Schoening^{63b}, P. G. Scholer⁵⁴, E. Schopf¹²⁵, M. Schott⁹⁹, J. Schovancova³⁶, S. Schramm⁵⁶, F. Schroeder¹⁶⁹, H.-C. Schultz-Coulon^{63a}, M. Schumacher⁵⁴, B. A. Schumm¹³⁵, Ph. Schune¹³⁴, A. Schwartzman¹⁴², T. A. Schwarz¹⁰⁵, Ph. Schwemling¹³⁴, R. Schwienhorst¹⁰⁶, A. Sciandra¹³⁵, G. Sciolla²⁶, F. Scuri^{73a}, F. Scutti¹⁰⁴, C. D. Sebastiani⁹¹, K. Sedlaczek⁴⁹, P. Seema¹⁸, S. C. Seidel¹¹¹, A. Seiden¹³⁵, B. D. Seidlitz⁴¹, T. Seiss³⁹, C. Seitz⁴⁸, J. M. Seixas^{81b}, G. Sekhniaidze^{71a}, S. J. Sekula⁴⁴, L. Selem⁴, N. Semprini-Cesari^{23a,23b}, S. Sen⁵¹, V. Senthilkumar¹⁶¹, L. Serin⁶⁶, L. Serkin^{68a,68b}, M. Sessa^{76a,76b}, H. Severini¹¹⁹, S. Sevova¹⁴², F. Sforza^{57a,57b}, A. Sfyrta⁵⁶, E. Shabalina⁵⁵, R. Shaheen¹⁴³, J. D. Shahinian¹²⁷, N. W. Shaikh^{47a,47b}, D. Shaked Renous¹⁶⁷, L. Y. Shan^{14a}, M. Shapiro^{17a}, A. Sharma³⁶, A. S. Sharma¹⁶², P. Sharma⁷⁹, S. Sharma⁴⁸, P. B. Shatalov³⁷, K. Shaw¹⁴⁵, S. M. Shaw¹⁰⁰, Q. Shen^{62c}, P. Sherwood⁹⁵, L. Shi⁹⁵, C. O. Shimmin¹⁷⁰, Y. Shimogama¹⁶⁶, J. D. Shinner⁹⁴, I. P. J. Shipsey¹²⁵, S. Shirabe⁶⁰, M. Shiyakova^{38.aj}, J. Shlomi¹⁶⁷, M. J. Shochet³⁹, J. Shojai¹⁰⁴, D. R. Shope¹⁴³, S. Shrestha¹¹⁸, E. M. Shrif^{33g}, M. J. Shroff¹⁶³, P. Sicho¹³⁰, A. M. Sickles¹⁶⁰, E. Sideras Haddad^{33g}, O. Sidiropoulou³⁶, A. Sidoti^{23b}, F. Siegert⁵⁰, Dj. Sijacki¹⁵, R. Sikora^{84a}, F. Sili⁸⁹, J. M. Silva²⁰, M. V. Silva Oliveira³⁶, S. B. Silverstein^{47a}, S. Simion⁶⁶, R. Simoniello³⁶, E. L. Simpson⁵⁹, N. D. Simpson⁹⁷, S. Simsek^{21d}, S. Sindhu⁵⁵, P. Sinervo¹⁵⁴, V. Sinetckii³⁷, S. Singh¹⁴¹, S. Singh¹⁵⁴, S. Sinha⁴⁸, S. Sinha^{33g}, M. Sioli^{23a,23b}, I. Siral¹²², S. Yu. Sivoklov^{37,*}, J. Sjölín^{47a,47b}, A. Skaf⁵⁵, E. Skorda⁹⁷, P. Skubic¹¹⁹, M. Slawinska⁸⁵, V. Smakhtin¹⁶⁷, B. H. Smart¹³³, J. Smiesko¹³², S. Yu. Smirnov³⁷, Y. Smirnov³⁷, L. N. Smirnova^{37.a}, O. Smirnova⁹⁷, E. A. Smith³⁹, H. A. Smith¹²⁵, J. L. Smith⁹¹, R. Smith¹⁴², M. Smizanska⁹⁰, K. Smolek¹³¹, A. Smykiewicz⁸⁵, A. A. Snesarev³⁷, H. L. Snock¹¹³, S. Snyder²⁹, R. Sobie^{163.v}, A. Soffer¹⁵⁰, C. A. Solans Sanchez³⁶, E. Yu. Soldatov³⁷, U. Soldevila¹⁶¹, A. A. Solodkov³⁷, S. Solomon⁵⁴, A. Soloshenko³⁸, K. Solovieva⁵⁴, O. V. Solovyanov³⁷, V. Solovyev³⁷, P. Sommer³⁶, A. Sonay¹³, W. Y. Song^{155b}, A. Sopczak¹³¹, A. L. Sapiro⁹⁵, F. Sopkova^{28b}, V. Sothilingam^{63a}, S. Sottocornola^{72a,72b}, R. Soualah^{115c}, Z. Soumami^{35e}, D. South⁴⁸, S. Spagnolo^{69a,69b}, M. Spalla¹⁰⁹, F. Spanò⁹⁴, D. Sperlich⁵⁴, G. Spigo³⁶, M. Spina¹⁴⁵, S. Spinalli⁹⁰, D. P. Spiteri⁵⁹, M. Spousta¹³², E. J. Staats³⁴, A. Stabile^{70a,70b}, R. Stamen^{63a}, M. Stamenkovic¹¹³, A. Stampekis²⁰, M. Standke²⁴, E. Stanecka⁸⁵, B. Stanislaus^{17a}, M. M. Stanitzki⁴⁸, M. Stankaityte¹²⁵, B. Stapf⁴⁸, E. A. Starchenko³⁷, G. H. Stark¹³⁵, J. Stark^{101.ah}, D. M. Starke^{155b}, P. Staroba¹³⁰, P. Starovoitov^{63a}, S. Stärz¹⁰³, R. Staszewski⁸⁵, G. Stavropoulos⁴⁶, J. Steentoft¹⁵⁹, P. Steinberg²⁹, A. L. Steinhebel¹²², B. Stelzer^{141,155a}, H. J. Stelzer¹²⁸, O. Stelzer-Chilton^{155a}, H. Stenzel⁵⁸, T. J. Stevenson¹⁴⁵, G. A. Stewart³⁶, M. C. Stockton³⁶, G. Stoicea^{27b}, M. Stolarski^{129a}, S. Stonjek¹⁰⁹, A. Straessner⁵⁰, J. Strandberg¹⁴³, S. Strandberg^{47a,47b}, M. Strauss¹¹⁹, T. Strebler¹⁰¹, P. Striznec^{28b}, R. Ströhmer¹⁶⁴, D. M. Strom¹²², L. R. Strom⁴⁸, R. Stroynowski⁴⁴, A. Strubig^{47a,47b}, S. A. Stucci²⁹, B. Stugu¹⁶, J. Stupak¹¹⁹, N. A. Styles⁴⁸, D. Su¹⁴², S. Su^{62a}, W. Su^{62c,62d,137}, X. Su^{62a,66}, K. Sugizaki¹⁵², V. V. Sulín³⁷, M. J. Sullivan⁹¹, D. M. S. Sultan^{77a,77b}

L. Sultanaliyeva³⁷, S. Sultansoy^{3b}, T. Sumida⁸⁶, S. Sun¹⁰⁵, S. Sun¹⁶⁸, O. Sunneborn Gudnadottir¹⁵⁹, M. R. Sutton¹⁴⁵, M. Svatos¹³⁰, M. Swiatlowski^{155a}, T. Swirski¹⁶⁴, I. Sykora^{28a}, M. Sykora¹³², T. Sykora¹³², D. Ta⁹⁹, K. Tackmann^{48,u}, A. Taffard¹⁵⁸, R. Tafirout^{155a}, J. S. Tafoya Vargas⁶⁶, R. H. M. Taibah¹²⁶, R. Takashima⁸⁷, K. Takeda⁸³, E. P. Takeva⁵², Y. Takubo⁸², M. Talby¹⁰¹, A. A. Talyshev³⁷, K. C. Tam^{64b}, N. M. Tamir¹⁵⁰, A. Tanaka¹⁵², J. Tanaka¹⁵², R. Tanaka⁶⁶, M. Tanasini^{57a,57b}, J. Tang^{62c}, Z. Tao¹⁶², S. Tapia Araya⁸⁰, S. Tapprogge⁹⁹, A. Tarek Abouelfadl Mohamed¹⁰⁶, S. Tarem¹⁴⁹, K. Tariq^{62b}, G. Tarna^{27b}, G. F. Tartarelli^{70a}, P. Tas¹³², M. Tasevsky¹³⁰, E. Tassi^{43a,43b}, A. C. Tate¹⁶⁰, G. Tateno¹⁵², Y. Tayalati^{35e}, G. N. Taylor¹⁰⁴, W. Taylor^{155b}, H. Teagle⁹¹, A. S. Tee¹⁶⁸, R. Teixeira De Lima¹⁴², P. Teixeira-Dias⁹⁴, J. J. Teoh¹⁵⁴, K. Terashi¹⁵², J. Terron⁹⁸, S. Terzo¹³, M. Testa⁵³, R. J. Teuscher^{154,v}, N. Themistokleous⁵², T. Theveneaux-Pelzer¹⁸, O. Thielmann¹⁶⁹, D. W. Thomas⁹⁴, J. P. Thomas²⁰, E. A. Thompson⁴⁸, P. D. Thompson²⁰, E. Thomson¹²⁷, E. J. Thorpe⁹³, Y. Tian⁵⁵, V. Tikhomirov^{37,a}, Yu. A. Tikhonov³⁷, S. Timoshenko³⁷, E. X. L. Ting¹, P. Tipton¹⁷⁰, S. Tisserant¹⁰¹, S. H. Tlou^{33g}, A. Tnourji⁴⁰, K. Todome^{23a,23b}, S. Todorova-Nova¹³², S. Todt⁵⁰, M. Togawa⁸², J. Tojo⁸⁸, S. Tokár^{28a}, K. Tokushuku⁸², R. Tombs³², M. Tomoto^{82,110}, L. Tompkins^{142,ai}, P. Tornambe¹⁰², E. Torrence¹²², H. Torres⁵⁰, E. Torró Pastor¹⁶¹, M. Toscani³⁰, C. Toscirci³⁹, D. R. Tovey¹³⁸, A. Traeet¹⁶, I. S. Trandafir^{27b}, T. Trefzger¹⁶⁴, A. Tricoli²⁹, I. M. Trigger^{155a}, S. Trincaz-Duvoid¹²⁶, D. A. Trischuk¹⁶², B. Trocmé⁶⁰, A. Trofymov⁶⁶, C. Troncon^{70a}, L. Truong^{33c}, M. Trzebinski⁸⁵, A. Trzupek⁸⁵, F. Tsai¹⁴⁴, M. Tsai¹⁰⁵, A. Tsiamis¹⁵¹, P. V. Tsiarehka³⁷, S. Tsigaridas^{155a}, A. Tsirigotis^{151,s}, V. Tsiskaridze¹⁴⁴, E. G. Tskhadadze^{148a}, M. Tsopoulou¹⁵¹, Y. Tsujikawa⁸⁶, I. I. Tsukerman³⁷, V. Tsulaia^{17a}, S. Tsuno⁸², O. Tsur¹⁴⁹, D. Tsybychev¹⁴⁴, Y. Tu^{64b}, A. Tudorache^{27b}, V. Tudorache^{27b}, A. N. Tuna³⁶, S. Turchikhin³⁸, I. Turk Cakir^{3a}, R. Turra^{70a}, P. M. Tuts⁴¹, S. Tzamarias¹⁵¹, P. Tzanis¹⁰, E. Tzovara⁹⁹, K. Uchida¹⁵², F. Ukegawa¹⁵⁶, P. A. Ulloa Poblete^{136c}, G. Unal³⁶, M. Unal¹¹, A. Undrus²⁹, G. Unel¹⁵⁸, K. Uno¹⁵², J. Urban^{28b}, P. Urquijo¹⁰⁴, G. Usai⁸, R. Ushioda¹⁵³, M. Usman¹⁰⁷, Z. Uysal^{21b}, V. Vacek¹³¹, B. Vachon¹⁰³, K. O. H. Vadla¹²⁴, T. Vafeiadis³⁶, C. Valderanis¹⁰⁸, E. Valdes Santurio^{47a,47b}, M. Valente^{155a}, S. Valentineti^{23a,23b}, A. Valero¹⁶¹, A. Vallier^{101,ah}, J. A. Valls Ferrer¹⁶¹, T. R. Van Daalen¹³⁷, P. Van Gemmeren⁶, S. Van Stroud⁹⁵, I. Van Vulpen¹¹³, M. Vanadia^{75a,75b}, W. Vandelli³⁶, M. Vandenbroucke¹³⁴, E. R. Vandewall¹²⁰, D. Vannicola¹⁵⁰, L. Vannoli^{57a,57b}, R. Vari^{74a}, E. W. Varnes⁷, C. Varni^{17a}, T. Varol¹⁴⁷, D. Varouchas⁶⁶, L. Varriale¹⁶¹, K. E. Varvell¹⁴⁶, M. E. Vasile^{27b}, L. Vaslin⁴⁰, G. A. Vasquez¹⁶³, F. Vazeille⁴⁰, T. Vazquez Schroeder³⁶, J. Veatch³¹, V. Vecchio¹⁰⁰, M. J. Veen¹¹³, I. Veliscek¹²⁵, L. M. Veloce¹⁵⁴, F. Veloso^{129a,129c}, S. Veneziano^{74a}, A. Ventura^{69a,69b}, A. Verbitskiy¹⁰⁹, M. Verducci^{73a,73b}, C. Vergis²⁴, M. Verissimo De Araujo^{81b}, W. Verkerke¹¹³, J. C. Vermeulen¹¹³, C. Vernieri¹⁴², P. J. Verschuur⁹⁴, M. Vessella¹⁰², M. L. Vesterbacka¹¹⁶, M. C. Vetterli^{141,ac}, A. Vgenopoulos¹⁵¹, N. Viaux Maira^{136f}, T. Vickey¹³⁸, O. E. Vickey Boeriu¹³⁸, G. H. A. Viehhauser¹²⁵, L. Vignani^{63b}, M. Villa^{23a,23b}, M. Villaplana Perez¹⁶¹, E. M. Villhauer⁵², E. Vilucchi⁵³, M. G. Vincter³⁴, G. S. Virdee²⁰, A. Vishwakarma⁵², C. Vittori^{23a,23b}, I. Vivarelli¹⁴⁵, V. Vladimirov¹⁶⁵, E. Voevodina¹⁰⁹, F. Vogel¹⁰⁸, P. Vokac¹³¹, J. Von Ahnen⁴⁸, E. Von Toerne²⁴, B. Vormwald³⁶, V. Vorobel¹³², K. Vorobev³⁷, M. Vos¹⁶¹, J. H. Vosseveld⁹¹, M. Vozak¹¹³, L. Vozdecky⁹³, N. Vranjes¹⁵, M. Vranjes Milosavljevic¹⁵, M. Vreeswijk¹¹³, R. Vuillermet³⁶, O. Vujanovic⁹⁹, I. Vukotic³⁹, S. Wada¹⁵⁶, C. Wagner¹⁰², W. Wagner¹⁶⁹, S. Wahdan¹⁶⁹, H. Wahlberg⁸⁹, R. Wakasa¹⁵⁶, M. Wakida¹¹⁰, V. M. Walbrecht¹⁰⁹, J. Walder¹³³, R. Walker¹⁰⁸, W. Walkowiak¹⁴⁰, A. M. Wang⁶¹, A. Z. Wang¹⁶⁸, C. Wang^{62a}, C. Wang^{62c}, H. Wang^{17a}, J. Wang^{64a}, P. Wang⁴⁴, R.-J. Wang⁹⁹, R. Wang⁶¹, R. Wang⁶, S. M. Wang¹⁴⁷, S. Wang^{62b}, T. Wang^{62a}, W. T. Wang⁷⁹, W. X. Wang^{62a}, X. Wang^{14c}, X. Wang¹⁶⁰, X. Wang^{62c}, Y. Wang^{62d}, Y. Wang^{14c}, Z. Wang¹⁰⁵, Z. Wang^{51,62c,62d}, Z. Wang¹⁰⁵, A. Warburton¹⁰³, R. J. Ward²⁰, N. Warrack⁵⁹, A. T. Watson²⁰, M. F. Watson²⁰, G. Watts¹³⁷, B. M. Waugh⁹⁵, A. F. Webb¹¹, C. Weber²⁹, M. S. Weber¹⁹, S. A. Weber³⁴, S. M. Weber^{63a}, C. Wei^{62a}, Y. Wei¹²⁵, A. R. Weidberg¹²⁵, J. Weingarten⁴⁹, M. Weirich⁹⁹, C. Weiser⁵⁴, C. J. Wells⁴⁸, T. Wenaus²⁹, B. Wendland⁴⁹, T. Wengler³⁶, N. S. Wenke¹⁰⁹, N. Wermes²⁴, M. Wessels^{63a}, K. Whalen¹²², A. M. Wharton⁹⁰, A. S. White⁶¹, A. White⁸, M. J. White¹, D. Whiteson¹⁵⁸, L. Wickremasinghe¹²³, W. Wiedenmann¹⁶⁸, C. Wiel⁵⁰, M. Wielers¹³³, N. Wieseotte⁹⁹, C. Wiglesworth⁴², L. A. M. Wiik-Fuchs⁵⁴, D. J. Wilbern¹¹⁹, H. G. Wilkens³⁶, D. M. Williams⁴¹, H. H. Williams¹²⁷, S. Williams³², S. Willocq¹⁰², P. J. Windischhofer¹²⁵, F. Winklmeier¹²², B. T. Winter⁵⁴, M. Wittgen¹⁴², M. Wobisch⁹⁶, A. Wolf⁹⁹, R. Wölker¹²⁵, J. Wollrath¹⁵⁸, M. W. Wolter⁸⁵, H. Wolters^{129a,129c}, V. W. S. Wong¹⁶², A. F. Wongel⁴⁸, S. D. Worm⁴⁸, B. K. Wosiek⁸⁵, K. W. Woźniak⁸⁵, K. Wraight⁵⁹, J. Wu^{14a,14d}, M. Wu^{64a}, S. L. Wu¹⁶⁸, X. Wu⁵⁶, Y. Wu^{62a}, Z. Wu^{62a,134}, J. Wuerzinger¹²⁵, T. R. Wyatt¹⁰⁰, B. M. Wynne⁵², S. Xella⁴², L. Xia^{14c}, M. Xia^{14b}, J. Xiang^{64c}, X. Xiao¹⁰⁵, M. Xie^{62a}

X. Xie^{62a}, J. Xiong^{17a}, I. Xiotidis¹⁴⁵, D. Xu^{14a}, H. Xu^{62a}, H. Xu^{62a}, L. Xu^{62a}, R. Xu¹²⁷, T. Xu¹⁰⁵, W. Xu¹⁰⁵, Y. Xu^{14b}, Z. Xu^{62b}, Z. Xu¹⁴², B. Yabsley¹⁴⁶, S. Yacoob^{33a}, N. Yamaguchi⁸⁸, Y. Yamaguchi¹⁵³, H. Yamauchi¹⁵⁶, T. Yamazaki^{17a}, Y. Yamazaki⁸³, J. Yan^{62c}, S. Yan¹²⁵, Z. Yan²⁵, H. J. Yang^{62c,62d}, H. T. Yang^{17a}, S. Yang^{62a}, T. Yang^{64c}, X. Yang^{62a}, X. Yang^{14a}, Y. Yang⁴⁴, Z. Yang^{62a,105}, W.-M. Yao^{17a}, Y. C. Yap⁴⁸, H. Ye^{14c}, J. Ye⁴⁴, S. Ye²⁹, X. Ye^{62a}, I. Yeletsikh³⁸, M. R. Yexley⁹⁰, P. Yin⁴¹, K. Yorita¹⁶⁶, C. J. S. Young⁵⁴, C. Young¹⁴², M. Yuan¹⁰⁵, R. Yuan^{62b,j}, X. Yue^{63a}, M. Zaazoua^{35e}, B. Zabinski⁸⁵, E. Zaid⁵², T. Zakareishvili^{148b}, N. Zakharchuk³⁴, S. Zambito⁵⁶, J. Zang¹⁵², D. Zanzi⁵⁴, O. Zaplatilek¹³¹, S. V. Zeißner⁴⁹, C. Zeitnitz¹⁶⁹, J. C. Zeng¹⁶⁰, D. T. Zenger Jr²⁶, O. Zenin³⁷, T. Ženiš^{28a}, S. Zenz⁹³, S. Zerradi^{35a}, D. Zerwas⁶⁶, B. Zhang^{14c}, D. F. Zhang¹³⁸, G. Zhang^{14b}, J. Zhang⁶, K. Zhang^{14a,14d}, L. Zhang^{14c}, R. Zhang¹⁶⁸, S. Zhang¹⁰⁵, T. Zhang¹⁵², X. Zhang^{62c}, X. Zhang^{62b}, Z. Zhang⁶⁶, H. Zhao¹³⁷, P. Zhao⁵¹, T. Zhao^{62b}, Y. Zhao¹³⁵, Z. Zhao^{62a}, A. Zhemchugov³⁸, Z. Zheng¹⁴², D. Zhong¹⁶⁰, B. Zhou¹⁰⁵, C. Zhou¹⁶⁸, H. Zhou⁷, N. Zhou^{62c}, Y. Zhou⁷, C. G. Zhu^{62b}, C. Zhu^{14a,14d}, H. L. Zhu^{62a}, H. Zhu^{14a}, J. Zhu¹⁰⁵, Y. Zhu^{62a}, X. Zhuang^{14a}, K. Zhukov³⁷, V. Zhulanov³⁷, N. I. Zimine³⁸, J. Zinsser^{63b}, M. Ziolkowski¹⁴⁰, L. Živković¹⁵, A. Zoccoli^{23a,23b}, K. Zoch⁵⁶, T. G. Zorbas¹³⁸, O. Zormpa⁴⁶, W. Zou⁴¹, L. Zwalinski³⁶

¹ Department of Physics, University of Adelaide, Adelaide, Australia

² Department of Physics, University of Alberta, Edmonton, AB, Canada

³ (a)Department of Physics, Ankara University, Ankara, Türkiye; (b)Division of Physics, TOBB University of Economics and Technology, Ankara, Türkiye

⁴ LAPP, Univ. Savoie Mont Blanc, CNRS/IN2P3, Annecy, France

⁵ APC, Université Paris Cité, CNRS/IN2P3, Paris, France

⁶ High Energy Physics Division, Argonne National Laboratory, Argonne, IL, USA

⁷ Department of Physics, University of Arizona, Tucson, AZ, USA

⁸ Department of Physics, University of Texas at Arlington, Arlington, TX, USA

⁹ Physics Department, National and Kapodistrian University of Athens, Athens, Greece

¹⁰ Physics Department, National Technical University of Athens, Zografou, Greece

¹¹ Department of Physics, University of Texas at Austin, Austin, TX, USA

¹² Institute of Physics, Azerbaijan Academy of Sciences, Baku, Azerbaijan

¹³ Institut de Física d'Altes Energies (IFAE), Barcelona Institute of Science and Technology, Barcelona, Spain

¹⁴ (a)Institute of High Energy Physics, Chinese Academy of Sciences, Beijing, China; (b)Physics Department, Tsinghua University, Beijing, China; (c)Department of Physics, Nanjing University, Nanjing, China; (d)University of Chinese Academy of Science (UCAS), Beijing, China

¹⁵ Institute of Physics, University of Belgrade, Belgrade, Serbia

¹⁶ Department for Physics and Technology, University of Bergen, Bergen, Norway

¹⁷ (a)Physics Division, Lawrence Berkeley National Laboratory, Berkeley, CA, USA; (b)University of California, Berkeley, CA, USA

¹⁸ Institut für Physik, Humboldt Universität zu Berlin, Berlin, Germany

¹⁹ Albert Einstein Center for Fundamental Physics and Laboratory for High Energy Physics, University of Bern, Bern, Switzerland

²⁰ School of Physics and Astronomy, University of Birmingham, Birmingham, UK

²¹ (a)Department of Physics, Bogazici University, Istanbul, Türkiye; (b)Department of Physics Engineering, Gaziantep University, Gaziantep, Türkiye; (c)Department of Physics, Istanbul University, Istanbul, Türkiye; (d)Istinye University, Sariyer, Istanbul, Türkiye

²² (a)Facultad de Ciencias y Centro de Investigaciones, Universidad Antonio Nariño, Bogotá, Colombia; (b)Departamento de Física, Universidad Nacional de Colombia, Bogotá, Colombia

²³ (a)Dipartimento di Fisica e Astronomia A. Righi, Università di Bologna, Bologna, Italy; (b)INFN Sezione di Bologna, Bologna, Italy

²⁴ Physikalisches Institut, Universität Bonn, Bonn, Germany

²⁵ Department of Physics, Boston University, Boston, MA, USA

²⁶ Department of Physics, Brandeis University, Waltham, MA, USA

²⁷ (a)Transilvania University of Brasov, Brasov, Romania; (b)Horia Hulubei National Institute of Physics and Nuclear Engineering, Bucharest, Romania; (c)Department of Physics, Alexandru Ioan Cuza University of Iasi, Iasi,

- Romania; ^(d)Physics Department, National Institute for Research and Development of Isotopic and Molecular Technologies, Cluj-Napoca, Romania; ^(e)University Politehnica Bucharest, Bucharest, Romania; ^(f)West University in Timisoara, Timisoara, Romania
- 28 ^(a)Faculty of Mathematics, Physics and Informatics, Comenius University, Bratislava, Slovak Republic; ^(b)Department of Subnuclear Physics, Institute of Experimental Physics of the Slovak Academy of Sciences, Kosice, Slovak Republic
- 29 Physics Department, Brookhaven National Laboratory, Upton, NY, USA
- 30 Departamento de Física, y CONICET, Facultad de Ciencias Exactas y Naturales, Instituto de Física de Buenos Aires (IFIBA), Universidad de Buenos Aires, Buenos Aires, Argentina
- 31 California State University, Long Beach, CA, USA
- 32 Cavendish Laboratory, University of Cambridge, Cambridge, UK
- 33 ^(a)Department of Physics, University of Cape Town, Cape Town, South Africa; ^(b)iThemba Labs, Cape Town, Western Cape, South Africa; ^(c)Department of Mechanical Engineering Science, University of Johannesburg, Johannesburg, South Africa; ^(d)National Institute of Physics, University of the Philippines Diliman, Quezon City, Philippines; ^(e)Department of Physics, University of South Africa, Pretoria, South Africa; ^(f)University of Zululand, KwaDlangezwa, Richards Bay, South Africa; ^(g)School of Physics, University of the Witwatersrand, Johannesburg, South Africa
- 34 Department of Physics, Carleton University, Ottawa, ON, Canada
- 35 ^(a)Faculté des Sciences Ain Chock, Réseau Universitaire de Physique des Hautes Energies-Université Hassan II, Casablanca, Morocco; ^(b)Faculté des Sciences, Université Ibn-Tofail, Kenitra, Morocco; ^(c)Faculté des Sciences Semlalia, Université Cadi Ayyad, LPHEA-Marrakech, Marrakech, Morocco; ^(d)LPMR, Faculté des Sciences, Université Mohamed Premier, Oujda, Morocco; ^(e)Faculté des sciences, Université Mohammed V, Rabat, Morocco; ^(f)Institute of Applied Physics, Mohammed VI Polytechnic University, Ben Guerir, Morocco
- 36 CERN, Geneva, Switzerland
- 37 Affiliated with an Institute Covered by a Cooperation Agreement with CERN, Geneva, Switzerland
- 38 Affiliated with an International Laboratory Covered by a Cooperation Agreement with CERN, Geneva, Switzerland
- 39 Enrico Fermi Institute, University of Chicago, Chicago, IL, USA
- 40 LPC, Université Clermont Auvergne, CNRS/IN2P3, Clermont-Ferrand, France
- 41 Nevis Laboratory, Columbia University, Irvington, NY, USA
- 42 Niels Bohr Institute, University of Copenhagen, Copenhagen, Denmark
- 43 ^(a)Dipartimento di Fisica, Università della Calabria, Rende, Italy; ^(b)INFN Gruppo Collegato di Cosenza, Laboratori Nazionali di Frascati, Frascati, Italy
- 44 Physics Department, Southern Methodist University, Dallas, TX, USA
- 45 Physics Department, University of Texas at Dallas, Richardson, TX, USA
- 46 National Centre for Scientific Research “Demokritos”, Agia Paraskevi, Greece
- 47 ^(a)Department of Physics, Stockholm University, Stockholm, Sweden; ^(b)Oskar Klein Centre, Stockholm, Sweden
- 48 Deutsches Elektronen-Synchrotron DESY, Hamburg and Zeuthen, Germany
- 49 Fakultät Physik, Technische Universität Dortmund, Dortmund, Germany
- 50 Institut für Kern- und Teilchenphysik, Technische Universität Dresden, Dresden, Germany
- 51 Department of Physics, Duke University, Durham, NC, USA
- 52 SUPA-School of Physics and Astronomy, University of Edinburgh, Edinburgh, UK
- 53 INFN e Laboratori Nazionali di Frascati, Frascati, Italy
- 54 Physikalisches Institut, Albert-Ludwigs-Universität Freiburg, Freiburg, Germany
- 55 II. Physikalisches Institut, Georg-August-Universität Göttingen, Göttingen, Germany
- 56 Département de Physique Nucléaire et Corpusculaire, Université de Genève, Geneva, Switzerland
- 57 ^(a)Dipartimento di Fisica, Università di Genova, Genoa, Italy; ^(b)INFN Sezione di Genova, Genoa, Italy
- 58 II. Physikalisches Institut, Justus-Liebig-Universität Giessen, Giessen, Germany
- 59 SUPA-School of Physics and Astronomy, University of Glasgow, Glasgow, UK
- 60 LPSC, Université Grenoble Alpes, CNRS/IN2P3, Grenoble INP, Grenoble, France
- 61 Laboratory for Particle Physics and Cosmology, Harvard University, Cambridge, MA, USA
- 62 ^(a)Department of Modern Physics and State Key Laboratory of Particle Detection and Electronics, University of Science and Technology of China, Hefei, China; ^(b)Institute of Frontier and Interdisciplinary Science and Key Laboratory of Particle Physics and Particle Irradiation (MOE), Shandong University, Qingdao, China; ^(c)Key Laboratory for Particle

- Astrophysics and Cosmology (MOE), SKLPPC, School of Physics and Astronomy, Shanghai Jiao Tong University, Shanghai, China; ^(d)Tsung-Dao Lee Institute, Shanghai, China
- 63 ^(a)Kirchhoff-Institut für Physik, Ruprecht-Karls-Universität Heidelberg, Heidelberg, Germany; ^(b)Physikalisches Institut, Ruprecht-Karls-Universität Heidelberg, Heidelberg, Germany
- 64 ^(a)Department of Physics, Chinese University of Hong Kong, Shatin, N.T., Hong Kong, China; ^(b)Department of Physics, University of Hong Kong, Hong Kong, China; ^(c)Department of Physics and Institute for Advanced Study, Hong Kong University of Science and Technology, Clear Water Bay, Kowloon, Hong Kong, China
- 65 Department of Physics, National Tsing Hua University, Hsinchu, Taiwan
- 66 IJCLab, Université Paris-Saclay, CNRS/IN2P3, 91405 Orsay, France
- 67 Department of Physics, Indiana University, Bloomington, IN, USA
- 68 ^(a)INFN Gruppo Collegato di Udine, Sezione di Trieste, Udine, Italy; ^(b)ICTP, Trieste, Italy; ^(c)Dipartimento Politecnico di Ingegneria e Architettura, Università di Udine, Udine, Italy
- 69 ^(a)INFN Sezione di Lecce, Lecce, Italy; ^(b)Dipartimento di Matematica e Fisica, Università del Salento, Lecce, Italy
- 70 ^(a)INFN Sezione di Milano, Milan, Italy; ^(b)Dipartimento di Fisica, Università di Milano, Milan, Italy
- 71 ^(a)INFN Sezione di Napoli, Naples, Italy; ^(b)Dipartimento di Fisica, Università di Napoli, Naples, Italy
- 72 ^(a)INFN Sezione di Pavia, Pavia, Italy; ^(b)Dipartimento di Fisica, Università di Pavia, Pavia, Italy
- 73 ^(a)INFN Sezione di Pisa, Pisa, Italy; ^(b)Dipartimento di Fisica E. Fermi, Università di Pisa, Pisa, Italy
- 74 ^(a)INFN Sezione di Roma, Rome, Italy; ^(b)Dipartimento di Fisica, Sapienza Università di Roma, Rome, Italy
- 75 ^(a)INFN Sezione di Roma Tor Vergata, Rome, Italy; ^(b)Dipartimento di Fisica, Università di Roma Tor Vergata, Rome, Italy
- 76 ^(a)INFN Sezione di Roma Tre, Rome, Italy; ^(b)Dipartimento di Matematica e Fisica, Università Roma Tre, Rome, Italy
- 77 ^(a)INFN-TIFPA, Povo, Italy; ^(b)Università degli Studi di Trento, Trento, Italy
- 78 Department of Astro and Particle Physics, Universität Innsbruck, Innsbruck, Austria
- 79 University of Iowa, Iowa City, IA, USA
- 80 Department of Physics and Astronomy, Iowa State University, Ames, IA, USA
- 81 ^(a)Departamento de Engenharia Elétrica, Universidade Federal de Juiz de Fora (UFJF), Juiz de Fora, Brazil; ^(b)Universidade Federal do Rio De Janeiro COPPE/EE/IF, Rio de Janeiro, Brazil; ^(c)Instituto de Física, Universidade de São Paulo, São Paulo, Brazil; ^(d)Rio de Janeiro State University, Rio de Janeiro, Brazil
- 82 KEK, High Energy Accelerator Research Organization, Tsukuba, Japan
- 83 Graduate School of Science, Kobe University, Kobe, Japan
- 84 ^(a)Faculty of Physics and Applied Computer Science, AGH University of Science and Technology, Kraków, Poland; ^(b)Marian Smoluchowski Institute of Physics, Jagiellonian University, Kraków, Poland
- 85 Institute of Nuclear Physics Polish Academy of Sciences, Kraków, Poland
- 86 Faculty of Science, Kyoto University, Kyoto, Japan
- 87 Kyoto University of Education, Kyoto, Japan
- 88 Research Center for Advanced Particle Physics and Department of Physics, Kyushu University, Fukuoka, Japan
- 89 Instituto de Física La Plata, Universidad Nacional de La Plata and CONICET, La Plata, Argentina
- 90 Physics Department, Lancaster University, Lancaster, UK
- 91 Oliver Lodge Laboratory, University of Liverpool, Liverpool, UK
- 92 Department of Experimental Particle Physics, Jožef Stefan Institute and Department of Physics, University of Ljubljana, Ljubljana, Slovenia
- 93 School of Physics and Astronomy, Queen Mary University of London, London, UK
- 94 Department of Physics, Royal Holloway University of London, Egham, UK
- 95 Department of Physics and Astronomy, University College London, London, UK
- 96 Louisiana Tech University, Ruston, LA, USA
- 97 Fysiska institutionen, Lunds universitet, Lund, Sweden
- 98 Departamento de Física Teórica C-15 and CIAFF, Universidad Autónoma de Madrid, Madrid, Spain
- 99 Institut für Physik, Universität Mainz, Mainz, Germany
- 100 School of Physics and Astronomy, University of Manchester, Manchester, UK
- 101 CPPM, Aix-Marseille Université, CNRS/IN2P3, Marseille, France
- 102 Department of Physics, University of Massachusetts, Amherst, MA, USA
- 103 Department of Physics, McGill University, Montreal, QC, Canada
- 104 School of Physics, University of Melbourne, Melbourne, VIC, Australia

- 105 Department of Physics, University of Michigan, Ann Arbor, MI, USA
106 Department of Physics and Astronomy, Michigan State University, East Lansing, MI, USA
107 Group of Particle Physics, University of Montreal, Montreal, QC, Canada
108 Fakultät für Physik, Ludwig-Maximilians-Universität München, Munich, Germany
109 Max-Planck-Institut für Physik (Werner-Heisenberg-Institut), Munich, Germany
110 Graduate School of Science and Kobayashi-Maskawa Institute, Nagoya University, Nagoya, Japan
111 Department of Physics and Astronomy, University of New Mexico, Albuquerque, NM, USA
112 Institute for Mathematics, Astrophysics and Particle Physics, Radboud University/Nikhef, Nijmegen, The Netherlands
113 Nikhef National Institute for Subatomic Physics and University of Amsterdam, Amsterdam, The Netherlands
114 Department of Physics, Northern Illinois University, DeKalb, IL, USA
115 (a) New York University Abu Dhabi, Abu Dhabi, United Arab Emirates; (b) United Arab Emirates University, Al Ain, United Arab Emirates; (c) University of Sharjah, Sharjah, United Arab Emirates
116 Department of Physics, New York University, New York, NY, USA
117 Ochanomizu University, Otsuka, Bunkyo-ku, Tokyo, Japan
118 Ohio State University, Columbus, OH, USA
119 Homer L. Dodge Department of Physics and Astronomy, University of Oklahoma, Norman, OK, USA
120 Department of Physics, Oklahoma State University, Stillwater, OK, USA
121 Joint Laboratory of Optics, Palacký University, Olomouc, Czech Republic
122 Institute for Fundamental Science, University of Oregon, Eugene, OR, USA
123 Graduate School of Science, Osaka University, Osaka, Japan
124 Department of Physics, University of Oslo, Oslo, Norway
125 Department of Physics, Oxford University, Oxford, UK
126 LPNHE, Sorbonne Université, Université Paris Cité, CNRS/IN2P3, Paris, France
127 Department of Physics, University of Pennsylvania, Philadelphia, PA, USA
128 Department of Physics and Astronomy, University of Pittsburgh, Pittsburgh, PA, USA
129 (a) Laboratório de Instrumentação e Física Experimental de Partículas-LIP, Lisbon, Portugal; (b) Departamento de Física, Faculdade de Ciências, Universidade de Lisboa, Lisbon, Portugal; (c) Departamento de Física, Universidade de Coimbra, Coimbra, Portugal; (d) Centro de Física Nuclear da Universidade de Lisboa, Lisbon, Portugal; (e) Departamento de Física, Universidade do Minho, Braga, Portugal; (f) Departamento de Física Teórica y del Cosmos, Universidad de Granada, Granada, Spain; (g) Instituto Superior Técnico, Universidade de Lisboa, Lisbon, Portugal
130 Institute of Physics of the Czech Academy of Sciences, Prague, Czech Republic
131 Czech Technical University in Prague, Prague, Czech Republic
132 Faculty of Mathematics and Physics, Charles University, Prague, Czech Republic
133 Particle Physics Department, Rutherford Appleton Laboratory, Didcot, UK
134 IRFU, CEA, Université Paris-Saclay, Gif-sur-Yvette, France
135 Santa Cruz Institute for Particle Physics, University of California Santa Cruz, Santa Cruz, CA, USA
136 (a) Departamento de Física, Pontificia Universidad Católica de Chile, Santiago, Chile; (b) Millennium Institute for Subatomic Physics at High Energy Frontier (SAPHIR), Santiago, Chile; (c) Instituto de Investigación Multidisciplinario en Ciencia y Tecnología, y Departamento de Física, Universidad de La Serena, La Serena, Chile; (d) Department of Physics, Universidad Andres Bello, Santiago, Chile; (e) Instituto de Alta Investigación, Universidad de Tarapacá, Arica, Chile; (f) Departamento de Física, Universidad Técnica Federico Santa María, Valparaiso, Chile
137 Department of Physics, University of Washington, Seattle, WA, USA
138 Department of Physics and Astronomy, University of Sheffield, Sheffield, UK
139 Department of Physics, Shinshu University, Nagano, Japan
140 Department Physik, Universität Siegen, Siegen, Germany
141 Department of Physics, Simon Fraser University, Burnaby, BC, Canada
142 SLAC National Accelerator Laboratory, Stanford, CA, USA
143 Department of Physics, Royal Institute of Technology, Stockholm, Sweden
144 Departments of Physics and Astronomy, Stony Brook University, Stony Brook, NY, USA
145 Department of Physics and Astronomy, University of Sussex, Brighton, UK
146 School of Physics, University of Sydney, Sydney, Australia
147 Institute of Physics, Academia Sinica, Taipei, Taiwan

- 148 (a)E. Andronikashvili Institute of Physics, Iv. Javakhishvili Tbilisi State University, Tbilisi, Georgia; (b)High Energy Physics Institute, Tbilisi State University, Tbilisi, Georgia; (c)University of Georgia, Tbilisi, Georgia
- 149 Department of Physics, Technion, Israel Institute of Technology, Haifa, Israel
- 150 Raymond and Beverly Sackler School of Physics and Astronomy, Tel Aviv University, Tel Aviv, Israel
- 151 Department of Physics, Aristotle University of Thessaloniki, Thessaloniki, Greece
- 152 International Center for Elementary Particle Physics and Department of Physics, University of Tokyo, Tokyo, Japan
- 153 Department of Physics, Tokyo Institute of Technology, Tokyo, Japan
- 154 Department of Physics, University of Toronto, Toronto, ON, Canada
- 155 (a)TRIUMF, Vancouver, BC, Canada; (b)Department of Physics and Astronomy, York University, Toronto, ON, Canada
- 156 Division of Physics and Tomonaga Center for the History of the Universe, Faculty of Pure and Applied Sciences, University of Tsukuba, Tsukuba, Japan
- 157 Department of Physics and Astronomy, Tufts University, Medford, MA, USA
- 158 Department of Physics and Astronomy, University of California Irvine, Irvine, CA, USA
- 159 Department of Physics and Astronomy, University of Uppsala, Uppsala, Sweden
- 160 Department of Physics, University of Illinois, Urbana, IL, USA
- 161 Instituto de Física Corpuscular (IFIC), Centro Mixto Universidad de Valencia-CSIC, Valencia, Spain
- 162 Department of Physics, University of British Columbia, Vancouver, BC, Canada
- 163 Department of Physics and Astronomy, University of Victoria, Victoria, BC, Canada
- 164 Fakultät für Physik und Astronomie, Julius-Maximilians-Universität Würzburg, Würzburg, Germany
- 165 Department of Physics, University of Warwick, Coventry, UK
- 166 Waseda University, Tokyo, Japan
- 167 Department of Particle Physics and Astrophysics, Weizmann Institute of Science, Rehovot, Israel
- 168 Department of Physics, University of Wisconsin, Madison, WI, USA
- 169 Fakultät für Mathematik und Naturwissenschaften, Fachgruppe Physik, Bergische Universität Wuppertal, Wuppertal, Germany
- 170 Department of Physics, Yale University, New Haven, CT, USA
- ^a Also Affiliated with an Institute Covered by a Cooperation Agreement with CERN, Geneva, Switzerland
- ^b Also at Borough of Manhattan Community College, City University of New York, New York, NY, USA
- ^c Also at Bruno Kessler Foundation, Trento, Italy
- ^d Also at Center for High Energy Physics, Peking University, Beijing, China
- ^e Also at Centro Studi e Ricerche Enrico Fermi, Rome, Italy
- ^f Also at CERN, Geneva, Switzerland
- ^g Also at Département de Physique Nucléaire et Corpusculaire, Université de Genève, Geneva, Switzerland
- ^h Also at Departament de Física de la Universitat Autònoma de Barcelona, Barcelona, Spain
- ⁱ Also at Department of Financial and Management Engineering, University of the Aegean, Chios, Greece
- ^j Also at Department of Physics and Astronomy, Michigan State University, East Lansing, MI, USA
- ^k Also at Department of Physics and Astronomy, University of Louisville, Louisville, KY, USA
- ^l Also at Department of Physics, Ben Gurion University of the Negev, Beersheba, Israel
- ^m Also at Department of Physics, California State University, East Bay, USA
- ⁿ Also at Department of Physics, California State University, Sacramento, USA
- ^o Also at Department of Physics, King's College London, London, UK
- ^p Also at Department of Physics, University of Fribourg, Fribourg, Switzerland
- ^q Also at Department of Physics, University of Thessaly, Vólos, Greece
- ^r Also at Department of Physics, Westmont College, Santa Barbara, USA
- ^s Also at Hellenic Open University, Patras, Greece
- ^t Also at Institutio Catalana de Recerca i Estudis Avancats, ICREA, Barcelona, Spain
- ^u Also at Institut für Experimentalphysik, Universität Hamburg, Hamburg, Germany
- ^v Also at Institute of Particle Physics (IPP), Toronto, Canada
- ^w Also at Institute of Physics, Azerbaijan Academy of Sciences, Baku, Azerbaijan
- ^x Also at Institute of Theoretical Physics, Ilia State University, Tbilisi, Georgia
- ^y Also at Lawrence Livermore National Laboratory, Livermore, USA
- ^z Also at Physics Department, An-Najah National University, Nablus, Palestine

^{aa} Also at The City College of New York, New York, NY, USA

^{ab} Also at The Collaborative Innovation Center of Quantum Matter (CICQM), Beijing, China

^{ac} Also at TRIUMF, Vancouver, BC, Canada

^{ad} Also at Università di Napoli Parthenope, Naples, Italy

^{ae} Also at University of Chinese Academy of Sciences (UCAS), Beijing, China

^{af} Also at Department of Physics, University of Colorado Boulder, Boulder, CO, USA

^{ag} Also at Physics Department, Yeditepe University, Istanbul, Türkiye

^{ah} Also at L2IT, Université de Toulouse, CNRS/IN2P3, UPS, Toulouse, France

^{ai} Also at Department of Physics, Stanford University, Stanford, CA, USA

^{aj} Also at Institute for Nuclear Research and Nuclear Energy (INRNE) of the Bulgarian Academy of Sciences, Sofia, Bulgaria

* Deceased